Deanship of Graduate Studies

Al-Quds University

Spectroscopic Study of the Interaction Effects of the Local Anesthetic Procaine [PRO] and Neurotransmitter in the Mammalian Central Nervous System Dopamine [DA] With Human Serum Albumin Protein [HSA].

Rania Abd Aljalel Sulaiman Fagyat

M.Sc. Thesis

Jerusalem –Palestine

1439 / 2018

Spectroscopic Study of the Interaction Effects of the Local Anesthetic Procaine [PRO] and Neurotransmitter in the Mammalian Central Nervous System Dopamine [DA] With Human Serum Albumin Protein [HSA].

Prepared by:

Rania Abd Aljalel Sulaiman Fagyat

B.Sc. Physics, Al-Quds University, Palestine.

Supervisor:

Prof. Musa Abu Teir

A thesis Submitted in Partial fulfillment of requirement for the degree of Master of Science from the Department of physics, Faculty of Science and Technology, Al-Quds University.

1439 / 2018

Al-Quds University

Deanship of Graduate Studies

Physics Department

Thesis Approval

Spectroscopic Study of the Interaction Effects of the Local Anesthetic Procaine [PRO] and Neurotransmitter in the Mammalian Central Nervous System Dopamine [DA] With Human Serum Albumin Protein [HSA].

Prepared by: Rania Abd Aljalel Sulaiman Fagyat

Registration No : 21420362

Supervisor: Prof. Musa Abu Teir.

Master Thesis submitted and accepted , Date: 15 / 4 / 2018

The names and signatures of the examining committee members are as follows:

1-Head of Committee: Prof. Musa Abutier Signature .....

2- Internal Examiner: Dr. Husain Alsamamra Signature .....

3-External Examiner: Dr. Adnan Judeh Signature .....

Jerusalem –Palestine

1439 / 2018

Dedication:

I dedicate this thesis to the sake of Allah, my Creator and my Master. My great teacher and messenger, Mohammed (May Allah bless and grant him) who taught us the purpose of life. My homeland Palestine, the warmest womb; the great martyrs and prisoners, the symbol of sacrifice. Alquds University; my second magnificent home. My great parents, who never stop giving of themselves in countless ways,. My dearest friend, Shireen, who leads me through the valley of darkness with light of hope and support, and stands by me when things look bleak. My friends whom I can't force myself to stop loving. My beloved brothers, Rafat and Rani, who are the symbol of love and giving. My sisters who stay with me all the time. My beloved uncle, Tayseer, who encourages and supports me all the time. All the people in my life who touch my heart, I dedicate this research.

Declaration:

I certify that this thesis submitted for the degree of Master is the result of my own research, except where otherwise acknowledged, and that this thesis (or any part of the same) has not been submitted for a higher degree to any other university or institution.

Signed: ----------

Rania Abd Aljalel Sulaiman Fagyat

Date: 15 / 4 / 2018.

Acknowledgements:

In the Name of Allah, the Most Merciful, the Most compassionate all praise be to Allah, the Lord of the worlds; and prayers and peace be upon Mohamed His servant and messenger. First and foremost, I must acknowledge my limitless thanks to Allah, the Ever-Magnificent; the Ever-Thankful, for His help and bless. I am totally sure that this work would have never become truth, without His guidance. I owe a deep debt of gratitude to our university for giving me an opportunity to complete this work. I am grateful to a person, who worked hard with me from the beginning till the completion of the present research Dr.Saqer Darwish, who has been always generous during all phases of the research, who told me that I can do what I want, who gave me all the force and the patience to do this research. Moreover, I highly appreciate the efforts expended by my supervisor Dr. Musa Abu Teir. I was very fortunate to have been able to work with him; his constant oversight of this thesis gave me the motivation to perform my maximum ability. Special thanks to Dr.Hussain Alsmmamreh, Dr.Imtiaz Darwish for their notes and help. I would like to take this opportunity to say warm thanks to all my beloved friends, who have been so supportive along the way of working on my thesis. I also would like to express my wholehearted thanks to my family [father, mother, sisters, and brothers] for their generous support they provided me throughout my entire life and particularly through the process of pursuing the master degree. Because of their unconditional love and prayers, I have the chance to complete this thesis. I owe profound gratitude to my best friend, Shireen, whose constant encouragement, limitless giving and great sacrifice, helped me accomplish my degree. I am very appreciative to my colleagues at Alquds University, who participated in this study.

Abstracts

It was found that the distribution and metabolism of many biologically active compounds in the body weather drugs or natural products are correlated with their affinities toward serum albumin. Thus; the study of the interaction of such molecules with albumin is of imperative and fundamental importance. Extensive studies on different aspects of drug-HSA interactions are still in progress because of the clinical significance of the processes.

In this study the interaction of Procaine (local anesthesia) and Dopamine (neurotransmitter in the mammalian central nervous system) with human serum albumin have been studied using UV-VIS spectrophotometer, fluorescence spectrophotometer, and FT-IR spectroscopy.

The results show that UV-absorption intensity was increased with the increase of procaine or Dopamine molar ratios in fixed amount of HSA. From UV spectra the binding constants were obtained and equals (1.00115599×10^3 M^{-1})for Procaine and (0 .849044×10^3 M^{-1}) for Dopamine.

The analysis of Fluorescence spectra indicated that Procaine and Dopamine have ability to quench the intrinsic Fluorcence of HSA through contribution of static and dynamic quenching procedure. The quenching rate constant values were determined to be 0.566×10^9 M^{-1}] for Procaine, and [$1 \cdot 04665 \times 10^9 M^{-1}$] for Dopamine .

The binding constants from Fluorescence spectrum for Procaine-HSA complexes were found to be [1.13818×10^3 M^{-1}], and for Dopamine-HSA complexes were found to be [0.88122×$10^3 M^{-1}$]. It was obviously noted that the obtained values agree well with the values obtained using UV-VIS spectrophotometer, and that procaine binding constant is larger than Dopamine binding constant, this refer to the structure of the two compounds which is consistent with that has been reported.

FT-IR spectroscopy with Fourier self-deconvolution and second derivative, as well as peak picking were used in the analysis of amide I, amide II, and amide III regions of HSA to determine protein secondary structure, Procaine, and Dopamine binding mechanism. It was observed that the intensity of absorption bands change after interaction between two drugs and HSA protein which indicate that the interaction and binding have taken place. Also all peak positions of the three amide regions were assigned at different Procaine or Dopamine ratios.

In addition, FT-IR spectra evidence showed that HSA secondary structure has been changed as Procaine or Dopamine molar ratios increased. The variation in the intensity is related indirectly to the formation of H-bonding in the complex molecules, which accorded for the different intrinsic propensities of α –helix and β –sheets.

Table of contents:

List of Tables:

List of Figures

List of Abbreviations:

Symbol	Abbreviation representation
HAS	Human Serum Albumin
UV-VIS spectrophotometer	Ultraviolet Visible spectrophotometer
FT-IR	Fourier Transform Infrared
α-helix	Alpha helix
β -sheet	Beta sheet
CD	Circular Dichroisms
FSD	Fourier Self Deconvolution
EM	Electromagnetic
ZPE	Zero-point energy
Kda	Kilodalton
OPUS	Optical User Software
Pro	Procaine
DA	Dopamine

List of Symbols a:

Symbol	Description
H	Planck's constant
F	Frequency
E_{tot}	Total energy
E_{ele}	Electronic energy
E_{vib}	Vibrational energy
E_{rot}	Rotational energy
K	Binding constant
r_0	Equilibrium position
Δx	Displacement
F_x	Restoring force
N	Number of molecule
n_i	Vibrational quantum numbers
V_{iv}	Potential energy of a harmonic oscillator
R	Distance between atoms
x_i	The anharmonicity constant
Q_i	Normal mode of vibration
n_i	Energy state
x_{ij}	Anharmonicity term introduces coupling between normal modes
1^{st} ,2^{nd}	First, Second
T	Transmittance
I	Radiant power transmitted by the sample
I_0	Radiation power incident on the sample
A	Absorbance
C, L	Concentrations
A	Absorptive
B	Pathlength
X	Optical path difference

Dv	Infinitesimal spectral signal
dF (x, v)	Interference signal
F(x)	The interference record
S_0, S_1, S_2	First, second, third states
K_{sv}	Stern Volmer quenching constant
K_q	Bimolecular quenching constant
τ_0	Unquenched lifetime
F_0	Fluorcence intensities without quencher
F	Fluorcence intensities with quencher
A_0	Initial absorption of protein
A_∞	Final absorption of the ligated-protein

Chapter one : Introduction

Local anesthesia is a drug which reversibly prevents the transmission of the nerve impulse where it is applied without affecting consciousness. Local anesthesias are divided into amide and ester classes as described in figure 1.2 . Historically, amide (lidocaine bupivacaine, Marcaine) and ester (procaine, tetracaine, Pontocaine) anesthetics were both used, but esters lost their favor after reports of increased sensitization(Covino et al., 1986).Chemical structure of local anesthesia is described in figure 1.1.

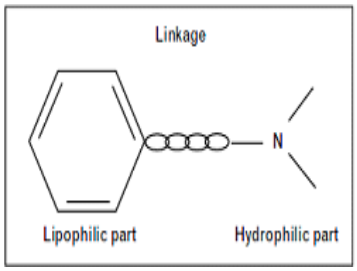

Figure1. 1.:Chemical structure of Local anesthesia.(Covino et al., 1986)

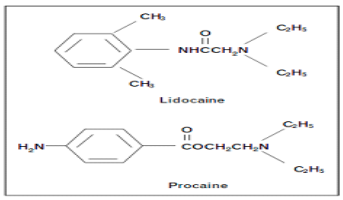

Figure1. 2: Amino acid and Amino acid ester Local anesthesia(Hara et al. , 2007)

Procaine is an ester local anesthetic used alone or with penicillin as an antibacterial drug. "Pro" has a chemical name of(2-diethyl aminoethyl-4-aminobenzoate hydrochloride) and its formula $C_{13}H_{20}N_2O_2$ with molecular weight of (272.8g/mole). Its chemical structure is described in figure (1.3). (Kahl et al., 2004)

Procaine and other local anesthetic drugs prevent the generation from the conduction of the nerve impulses. Their main action site is the cell membrane since conduction block can

be demonstrated in giant axons from which the exoplasm has been removed.(Hara et al., 2007; Kahl et al., 2004).

Procaine is used in obstetrics and sometimes for relieving pain in the lower back and tooth extraction.(Malamed et al., 2001) ."Pro" shows a short duration of action and adverse side effects, such as cardiac and neurological toxicity. Its short action is exerted by its storage in proteins and transportation by proteins in blood plasma.(Xie et al., 2015).

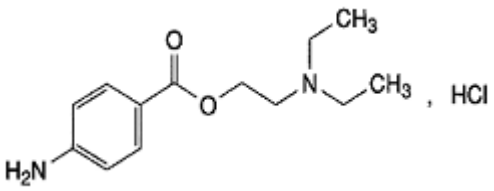

Figure1. 1: Chemical Structure of Procaine. (Racine et al., 1975; Xie et al., 3 .Figure1 2015)

Dopamine is a major neurotransmitter in the mammalian central nervous system. It's involved in the control of the locomotors activity and also in the pathways that regulate pleasure and reward-seeking behavior.(Bäckman et al., 2010).Parkinson’s disease is a degenerative ailment of the central nervous system. Its symptoms can be treated with medication that increases the dopamine level in the brain. Also, in the past few decades, there has been a serious debate on the role of dopamine in drug addiction. Now, it is generally accepted that this substance is pivotal in the development and persistence of the addiction.(Bäckman et al., 2010; Bergin et al.,1968; Q. Zhang et al.,2012)

In general, dopamine (DA) is related to the overstimulation of emotions, pleasure, and reward systems. The repeated experience of which, via drug taking, facilitates the development of craving patterns, that is, drug addiction .(Chen et al., 2003)

Dopamine Hydrochloride is chemically designated 3, 4-dihydroxyphenethylamine hydrochloride and its formula is (C8H11NO2 • HCl).its chemical structure described in figure (1.4). A white crystalline powder freely soluble in water. It has the following structural formula(Ungless et al., 2010).

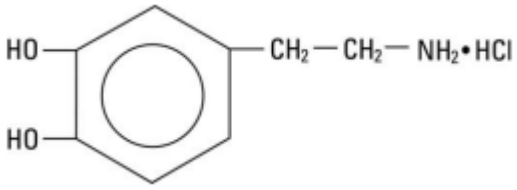

Figure1. 4:Chemical Structure of Dopamine.(Young et al., 2011).

Human serum albumin which is denoted by (HSA) is a major and most abundant prominent protein found in plasma, it is synthesized in the liver and accounts for at least 10% of liver protein synthesis. Its physiological and pharmacological properties have been extensively studied over several decades.(H. Zhang et al., 2008).

HSA is best known for its extraordinary ligand binding capacity. Also, it has a high affinity to a very wide range of endogenous and exogenous ligand and materials, including metals such as Cu^{2+} and Zn^{2+}, fatty acids, amino acids, metabolites such as bilirubin and for many drug compounds.(Bhattacharya et al., 2000)**.**The most important physiological role of the protein is to move such solutes into the bloodstream to their target organ in addition to its role in transporting the endogenous and exogenous ligands.(He et al., 2005)**.**

The drugs distribution, metabolism, and efficacy and the biologically active compounds can be altered on the basis of their affinity to serum albumin. Significantly as shown in figure (1.5), the determination and understanding of dopamine’s and procaine's

interacting with serum albumin is crucial for the therapy and the design of the drug (Young et al., 2011).

The interaction knowledge and its binding to HSA does not only give information on the pharmacological action of that drugs and illuminates its binding mechanism, but it also provides guidance on whether the role of dopamine and procaine is restricted to the reward-addiction state or to any possible alternative explanations especially to the inconsistent findings on dopamine and procaine drug addiction.(Zhang et al., 2012).

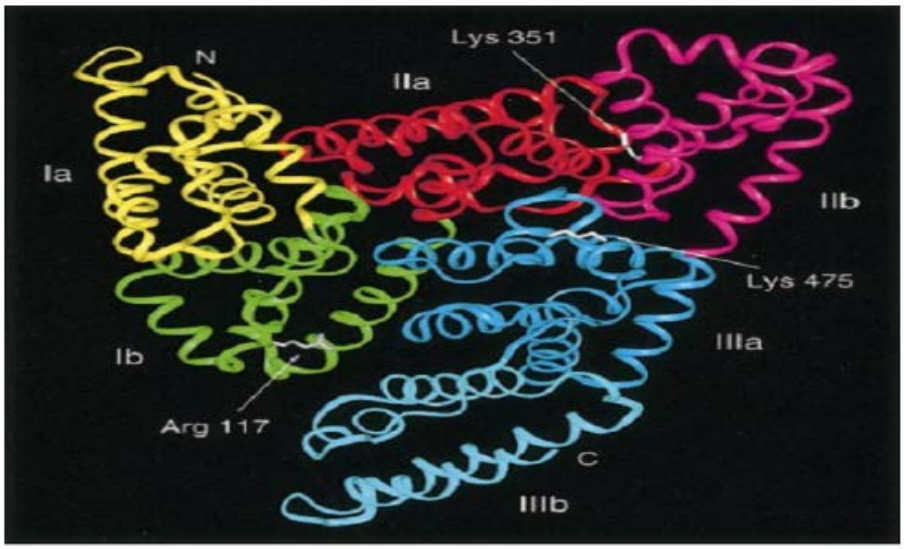

Figure1. 5-: Schematic drawing of the HSA molecule. Each sub domain is marked with a different color (yellow for sub domain Ia; green, Ib ; red, IIa; magenta, IIIb; blue, IIa; and cyan, IIIb).(Khan et al., 2008).

The molecular interactions between HSA and some compounds have been investigated successfully.(Stan et al., 2009). (Lupidi et al.,2010) evaluated the interactions between TQ and HSA by various spectroscopic techniques. A research carried out by Tajmir-Riahi (Tajmir et al ., 2007) studied various drugs binding to high concentrations of HSA, and determined the effects of drug complexion on protein secondary confirmation.

(Bia et al., 2009) presented a study about the interaction of HSA with phenothiazine drugs by using fluorescence quenching and differentiation between static and dynamic quenching. (Moosavi et al.,2006)determined the interaction of HSA with bilirubin**.** (Sugio et al., 1999) studied the effects of acyclovir and triton–X-100 on the behavior of HSA by many spectroscopic techniques.

The interaction of alpinetin with HSA was studied by (He et al.,2005) and by many spectroscopy techniques such as Fourier transform infrared spectroscopy, fluorescence quenching and U.V. absorption spectroscopy and circular dichroism. (Li et al., 2011) studied the binding between plumbagin to HSA in physiological conditions by fluorescence spectroscopy.(Bai et al., 2009)studied the interaction between the sinomenine and Bovine Serum Albumin (BSA) by fluorescence spectra, Fourier Transform-Infrared and Circular Dichroism spectroscopy.

(Stan et al., 2009), investigated the binding parameters (binding constants and number of binding sites) and quenching constants for the interaction of new indanedione derivatives with HSA and Bovine Serum Albumin (BSA) by fluorescence technique. A study performed by (Krisko et al., 2005)to investigate the binding of caffeine to HSA based on the application of fluorescence spectroscopy. And they estimated the binding constant of this interaction.

(Khan et al., 2008)studied the binding of thiopental with HSA by UV absorption and fluorescence spectroscopy.

In recent years, many investigations on drugs and natural products binding to protein have been carried out. Procaine's interaction with HSA was studied via using a multi-way calibration method coupled with three-dimensional fluorescence spectroscopy(Xie et al., 2015).That investigation reported that procaine binds to HSA.

Dopamine's interaction with bovine serum albumin (BSA) was studied by different spectroscopic techniques. In addition, a fluorescence quenching mechanism was associated with this process. Estimated thermodynamic parameters indicated the presence of hydrogen bonding and van der Walls forces between dopamine and BSA. (Q. Zhang et al., 2012).That investigation reported that DA binds to BSA and since BSA is an album in protein such as HSA, I predicted that DA may bind HSA.

In this thesis, the interaction of procaine and dopamine with HSA will be investigated in details by means of three different spectroscopy FT-IR, UV-VIS, and fluorescence spectrophotometer to determine in details the Pro-HSA, and DA-HSA binding constants and the effects of Pro or DA complexation on the protein structure.

Infrared spectroscopy provides measurements of molecular vibrations due to the specific absorption of infrared radiation by chemical bonds .Its known that the form and frequency of the amide I band, which is assigned to C==O stretching vibration within the peptide bonds is very characteristic for the structure of the studied protein from the band secondary structure, components peaks $(\alpha - he\ell ix, \beta - sheets)$ can be derived and the analysis of this single band allows elucidation of conformational changes with high sensitivity (Darwish et al.,2010).

This work will be limited to the mid-range infrared, which covers the frequency range from 4000 to $400\,cm^{-1}$.This wavenumber region includes bands that arise from three conformational sensitive vibrations within the peptide backbone [Amide I, II, and III]. Amide I is the most widely used and can provide information on secondary structure composition and structural stability .However , it has been reported that amide II and amide III bands have high information content and could be used for prediction of proteins secondary structure .(Abu Teir et al., 2012).

It has recently been proved that serum albumin plays a decisive role in the transport and disposition of a variety of endogenous and exogenous such as fatty acids, hormones, drugs(Abu Teir et al., 2011).Another spectroscopic technique is usually used in studying drugs interact with proteins, such as fluorescence and UV-VIS spectrophotometer which is commonly used due to their high sensitivity, rapidity, and ease of implementation (Saleh et al., 2003).

Beside this chapter, four chapters will be covered in this thesis. Chapter two will discuss the theoretical aspects and the important ideas of this study. Chapter three discuss the experimental, procedures, and instrumental devices that used in our study. Chapter four shows and discussed the results that have been obtained. And the last chapter is about the conclusions and future work.

Theoretical Background: Theoretical Background

Biophysics is a branch of science which uses and applies physics, Biology, chemistry, mathematical equations and computer model. These are used to study, to analyze and to explain how the biological system works. We can consider this science as the bridge between physics, chemistry, and biology. Biophysics is a molecular science which dramatically ranges from small fatty acid and sugars to macromolecules, such as protein.

Biophysics seeks for explaining the biological function in terms of molecular structure and biological interaction using the spectroscopic techniques of physics and chemistry. The relationship between both the biological function and the molecular structure is investigated via using highly precise and exquisitely sensitive physical instruments and techniques.

Research in Biophysics had been started for first time in India in the late of the nineteenth century when the renowned physicist J.C. Bose began his pioneering work on the behavior of cells under external stimuli. Nowadays, more than a hundred research groups distributed in different institutions around the world are engaged in research in the field of Biophysics. Among them, they cover almost all aspects of biophysics, especially at the molecular level.

The spectrophotometer is one of the instruments and techniques that are used to study the biological interaction system and its function such as protein this chapter will cover theoretical aspects of this research. The first two sections will include and contain the development of this technique whereas the second will discuss the electromagnetic spectrum. The next section will briefly cover the molecular vibration. The other three sections will discuss the spectroscopic techniques I adopted in this work. They are FT-IR, UV-VIS, and Fluorescence one. The last chapter includes protein structure and protein mode that I used as a 'Human Serum Albumin (HSA)"

2.1 Fourier Transform Infrared Spectroscopy (FT-IR) development

Spectroscopy is a study of interaction between matter and electromagnetic radiation. When matter absorbs radiation, its molecules excited to higher molecular vibrational state. The probability of interaction between matter and electromagnetic radiation depends on the interaction between actual frequency and matter. Since each material is unique in its atom components, there are no two compounds that can produce the same spectrum.

Therefore, we can consider spectroscopic technique as a fingerprint and a qualitative analysis technique. Also, the size of the peaks can be considered as an indicator to the quantity of material where its peaks could be noticed by interaction of radiation with it. In the spectroscopic technique, the researcher carried out both the quantitative and the qualitative technique as tools of the study.(Sathyanarayana et al., 2015)

Fourier Transform spectroscopy is a general term that describes the analysis of any varying signal into its constitute frequencies component. FTS can for many spectroscopes include infrared spectroscopy, nuclear magnetic and electron spin resonance spectroscopy (Stuart et al., 2004). FTS can be used for a long range of frequencies varying from ultraviolet range to far infrared regions.

In FT spectroscopy, the samples don't expose to varying energy of an electromagnetic radiation. It is exposed to a signal pulse of radiation consisting of frequency in particular range. When the interaction occurs between specific energy radiation and the sample, the energy will be absorbed resulting in a series of peaks in the spectrum signal corresponding to the frequencies of vibrations between the bonds of the atoms making up the material.(Rosén et al., 2010).

FTIR spectroscopy is a strong and a powerful analytical spectroscopic technique that is used to study and to analyze the biological system structure, interactions, and functions. A good example for this is the protein system which studies the spectrum that appears during the electromagnetic radiation in the IR region interaction with the biological system. By determining what fraction of the incident radiation is absorbed in a particular energy.(Stuart et al., 2004).

The energy spectrum where its absorption reaches its peak corresponds to the frequency of the vibration of the molecule sample. Then, we can get much information of that system such as band positions, bandwidth, absorption, an investigation of protein folding, unfolding and other protein structural changes that occur during molecular interactions.(Stuart et al., 2005).

The Fourier transform science began in the late of the 1880s when Albert Michelson invented the first interferometer which was known as Michelson interferometer. He was able to do his famous experiment and to determine the speed of light. The lack of the sensitive detectors, the Fourier nonexistence and the algorithm transform were the main barriers. Due to its practical applications, in the late of 1940s Fourier came to the scene when scientists used interferometer to determine the light from celestial in 1994 the first Fourier transform spectrum was produced .(Markovich et al., 1991).

At the onset of 1960, the interest of interferometry spectroscopy was gradually increased in addition to its applications in physics started to appear. In 1969, the first near-infrared planetary spectra were recorded. Later, in 1969 high resolution and high-quality spectra of the planets were measured. By 1970, FTS started to be the invaluable tool for the researches.(Kast et al., 2015).

The first FT-IR spectrometer was huge, expensive, and difficult to use, and primarily found in a well-to-do research laboratory. Today, technology is reducing the cost, increasing the availability, and enhancing the capabilities of FT-IR spectrometers. Moreover, developed and fast computer are currently added to FTS. This performs Fourier transformation in the fraction of a second in the visible, infrared, and microwave regions that are common in the laboratory instruments.(Ferrari et al., 2012).

2.2 Electromagnetic Radiation

Optical Spectroscopy is an analytical technique used to study the interaction between matter and electromagnetic radiation. It is called "optical technique" because it uses an optical material to disperse and focus the radiation on the intended matter .(Henderson et al., 2006).

The Electromagnetic radiation can be defined as a form of energy that consists of oscillating electric and magnetic field which propagate along a linear path. Also, the constant velocity of c $(3\times10^{8}\,m/s)$ when that radiation moves in a vacuum, and velocity of **v** which is less than c when it moves through a medium.

Electric and magnetic field oscillation is perpendicular to each other and to the direction of wave's propagation, Figure (2-1) shows an example of plane-polarized electromagnetic radiation, consists of a single oscillating electric field and a single oscillating magnetic field.(Stedwell et al., 2013).

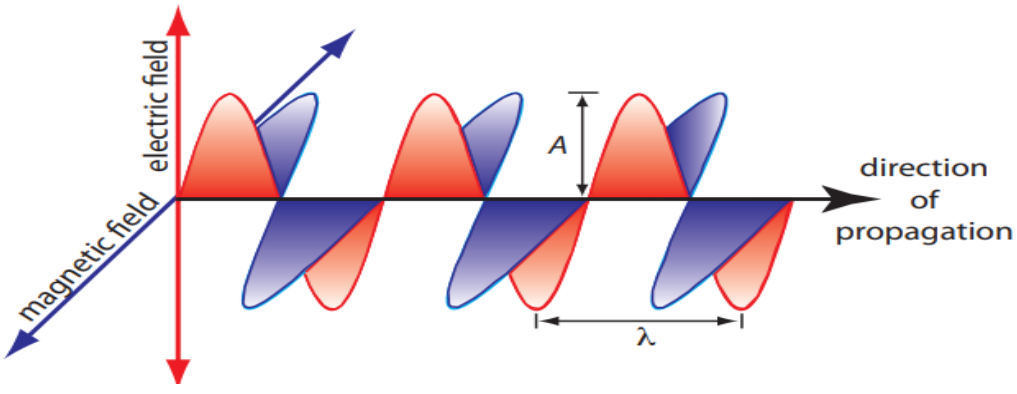

Figure2. 1:Plane-polarized electromagnetic radiation showing the oscillating electric field in red and the oscillating magnetic field in blue. The radiation's amplitude, A, and its wavelength, λ, are shown.(Stedwell et al., 2013).

The Electromagnetic radiation show proprieties of both wave and particle known as the wave-particle duality, in the wave model electromagnetic radiation described by its frequency f, wavelength λ, and velocity c. These characteristics are related to each other by the equation (1).(Harvey et al., 2000)

$$c = \lambda f \ldots\ldots\ldots (1)$$

Under certain conditions, the electromagnetic radiation shows particle-like nature that is called a photon. Thus, it's useful to describe electromagnetic radiation as the packet of energy (Harveyet al., 2000; Stedwell et al., 2013).

Albert Einstein put equation (2) which describes the relationship between photon's energy, the frequency, and the wavelength as below:

$$E = \frac{hc}{\lambda} = hf \ldots\ldots\ldots (2).$$ Where h is plank's constant

When all kinds of different electromagnetic radiations come close to each other, they form different regions of different wavelength and various corresponding energy called electromagnetic spectrum. Each region of that energy corresponds and used for different spectroscopic techniques.(Wilson et al., 2010).

The extent of electromagnetic spectrum from low- energy radio wave to high energy – gamma rays radiation is illustrated in figure (2-2).

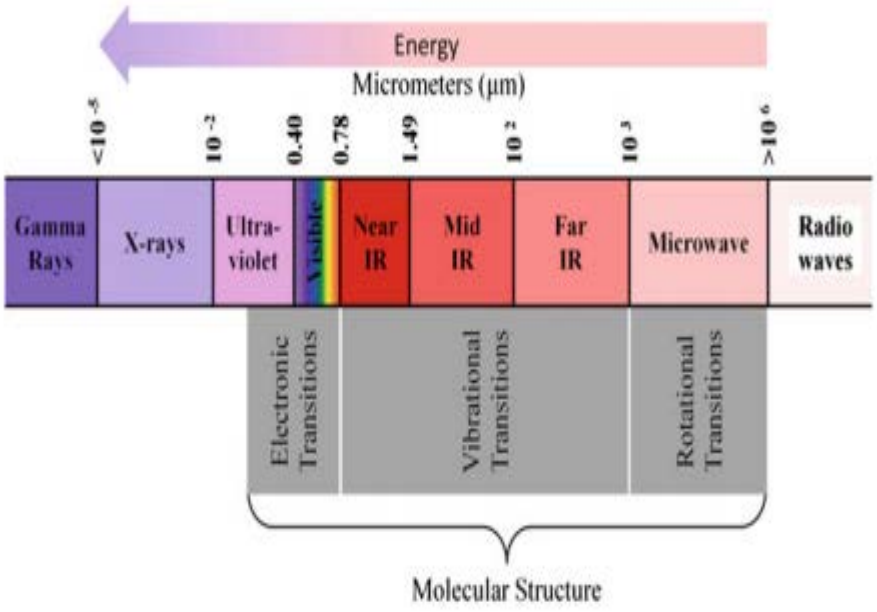

Figure2. 2: The electromagnetic spectrum covers a continuous range of wavelengths, from low energy radio waves to gamma (c) rays at the high-energy end.(Wilson et al., 2010).

The microwave region of the electromagnetic spectrum is associated with rotational spectroscopy, while the UV and Visible portions correspond to molecular electronic transitions. On another hand, The IR region, which is typically broken into near, mid, and far-IR, is utilized in vibrational spectroscopy .(Kerker et al., 2016).

Figure (2-3) shows electromagnetic spectrum and its usage for spectroscopic methods.

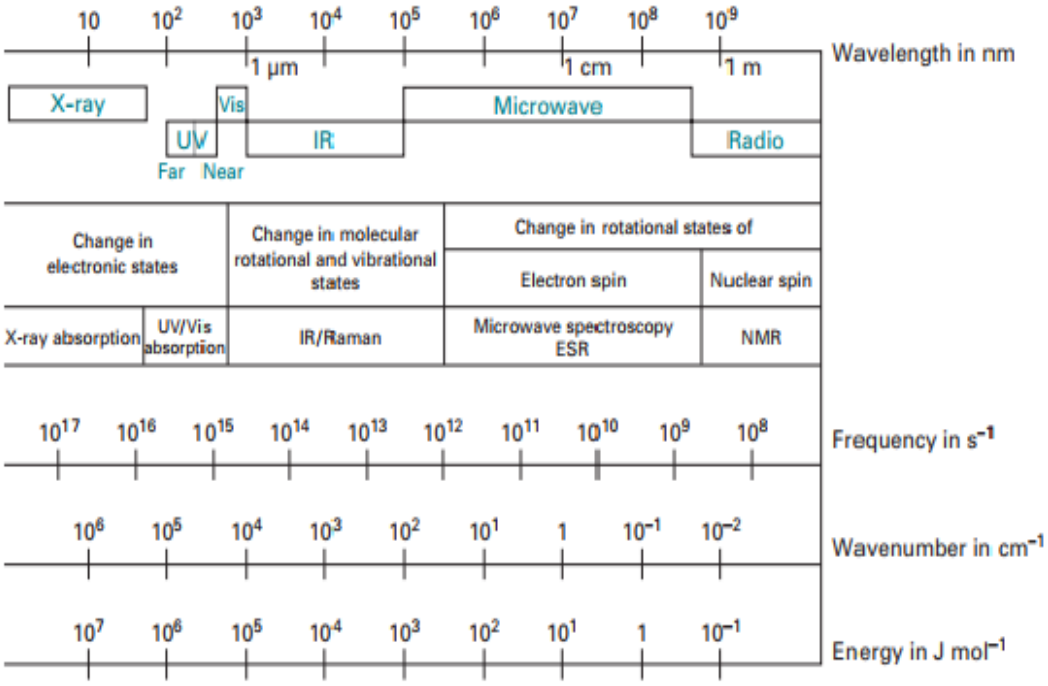

Figure2. 3: The electromagnetic spectrum and its usage for spectroscopic methods (Henderson et al.,2006).

2.3 Molecular Vibration

IR Spectroscopy is the analytical technique based on the atom's vibration of the molecule. When IR radiation passes through the sample fraction, an incident radiation at a particular frequency is absorbed.(Backx et al.,1977). As a result of this absorption, IR spectrum is obtained.

There are two general types of molecular vibration: stretching and bending. Stretching is the rhythmical movement along the bond axis and can be symmetric or anti symmetric. Bending vibrations arise from a change in bond angle between two atoms or movement of a group of atoms, relative to the remainder of the molecule.(Gao et al., 1998).

In stretching vibration, the frequency of a bond can be approximated via using Hooke's law as shown in wquation (3). This approximation treats the two masses and the connecting bond as a simple harmonic oscillator. It assumes that the two masses represent the atoms joined by a spring that represents the chemical bond; figure (2-4) illustrates simple harmonic approximation for diatomic molecules .(Djukic et al., 2005)

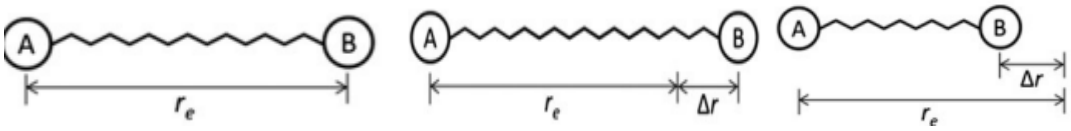

Figure2. 4:Motions of a diatomic oscillator AB.(Djukic et al ., 2005).

$F = -K\Delta r$ …… 3 , where k is the force constant.

When the restoring force causes the molecular motion to cease, the atom will begin moving in the opposite direction. This creates a smooth oscillatory motion known vibration.

The frequency of vibration related to the mass and the force constant of the spring are illustrated by equation (4).

$$\nu = \frac{1}{2\pi}\sqrt{\frac{k}{\mu}} \ldots\ldots\ldots\ldots (4)$$,where μ is the reduced mass $\mu = \frac{m_a m_b}{m_a + m_b}$

In the classical harmonic osillciator, the energy of vibration given by equation (5) .

$$E = \frac{1}{2} K\Delta r^2 = h\nu \ldots\ldots\ldots\ldots (5)$$

According to the last two equations, we can consider that the energy or frequency depends on how far one stretches or compresses the spring. If we look to equation (5) in a classical view, we can see that any value of r is possible and since this model is true, molecule can absorb any value of wavelength .(Dekker et al , 1981).

2.3.1 Normal mode of vibration:

Normal modes are the pattern of motion in which all parts of the molecule move sinusoidal with the same frequency and with the fixed phase relation These modes vibrate independently and don't interfere with each other [mathematically they form orthonormal basis.(Mills et al., 1985).

The number of the normal mode is equal to the degree of freedom in the Cartesian coordinate. In Cartesian coordinate system, each atom can be displaced in the x- , y-, and z- directions corresponding to three degrees of freedom, Thus for 3D molecules with N atoms, there will be 3N normal modes , but not all for vibrational mode, three of them will be transitional mode, T_X, T_Y, T_Z three will be rotational $R_X R_Y R_Z$ in nonlinear molecule, while only two transitional modes in the linear molecule are required, the remaining 3N-6 will be vibrational mode that is denoted by v_i where i=3N-6 for nonlinear molecule and 3N-5 mode (degree of freedom)for linear one.(Banwell et al., 1994).

The degree of freedom for polyatomic molecule, i.e. linear or nonlinear are summarized in table (2-1)

Table2. 1: Degree of freedom for polyatomic molecule.(Banwell et al,. 1994).

	Linear	Nonlinear
Translational degrees of freedom	3	3
Rotational degrees of freedom	2	3
Vibrational degrees of freedom	3N - 5	3N -6

2.3.2 Quantuem meechanical tretment of vibration:

I-The harmonic approximation:

According to the classical mechanics, a harmonic oscillator may vibrate with any amplitude. This means that it can have any amount of energy and large or small quantum mechanics. However, it shows that molecules can only exist in definite energy states [energy is quantized].(Ipnl et al., 2008).

The quantum mechanical Hamiltonian for a one-dimensional harmonic oscillator and the Schrödinger equation are below given in the equations (7, 8).

$$H = -\frac{\hbar}{2\mu}\frac{d^2}{dx^2} + \frac{1}{2}KX^2 \ldots\ldots (6) \qquad \frac{d^2\psi_v}{dx^2} + (\frac{2\mu E_V}{\hbar^2} - \frac{\mu k x^2}{\hbar^2})\Psi_V = 0 \ldots.(7)$$

Solving Schrodenger equation the energy state for harmonic potential will be described as equation (8).

$$E_V = h\nu(n_i + \frac{1}{2}) \ldots\ldots\ldots (8)$$

Where n_i is the vibrational quantum number which can take only positive integer values including zero, h is Planck's constant. The potential energy of harmonic oscillator is shown by the dashed line in figure (2-5) as a function of the distance between the atoms r.

II –Anharmonicity:

The bond in real molecules disagrees with Hooke's law. When the two atoms approach each other, there must be a repulsive force between them. Thus, the vibrational energy will increase very rapidly and the molecule will deviate from harmonistic. The two atoms go far away from each other and the bond between them will be broken.(Herzberg et al., 2013).

The vibrational energy equals the dissociation energy. The actual variation of the potential energy as a function of the displacement of the atoms from their equilibrium positions is shown as the solid line in figure (2-5). The anharmonicity can be calculated by using the perturbation theory. The vibrational energy for diatomic molecule must be modified to apply the anharmonicity(Townes et al.,2013). The function which represents this is the Morse Function used in equation (9) as below:

$$E = D_{eq}[1-\exp\{a(r_{eq}-r)\}]^2 \ldots\ldots\ldots \quad (9)$$

Where D_{eq} is the dissociation energy, which is constant for a particular molecule,r_{eq} is the equilbruim distance , a is the amplitude and r is the stretching distance

Using perturbation theory, the vibrational energy described in equation (10) .

$$E_V = (v+\frac{1}{2}w_e \_(v+\frac{1}{2}w_e\chi_e) \ldots\ldots\ldots\ldots (10)$$

Where w_e the oscillation frequency is expressed in wavenumbers and χ_e is the anharmonicity constant (Henry et al., 1968).

Both of harmonic and anharmonic approximation of molecular vibration is described in figure 2.5:

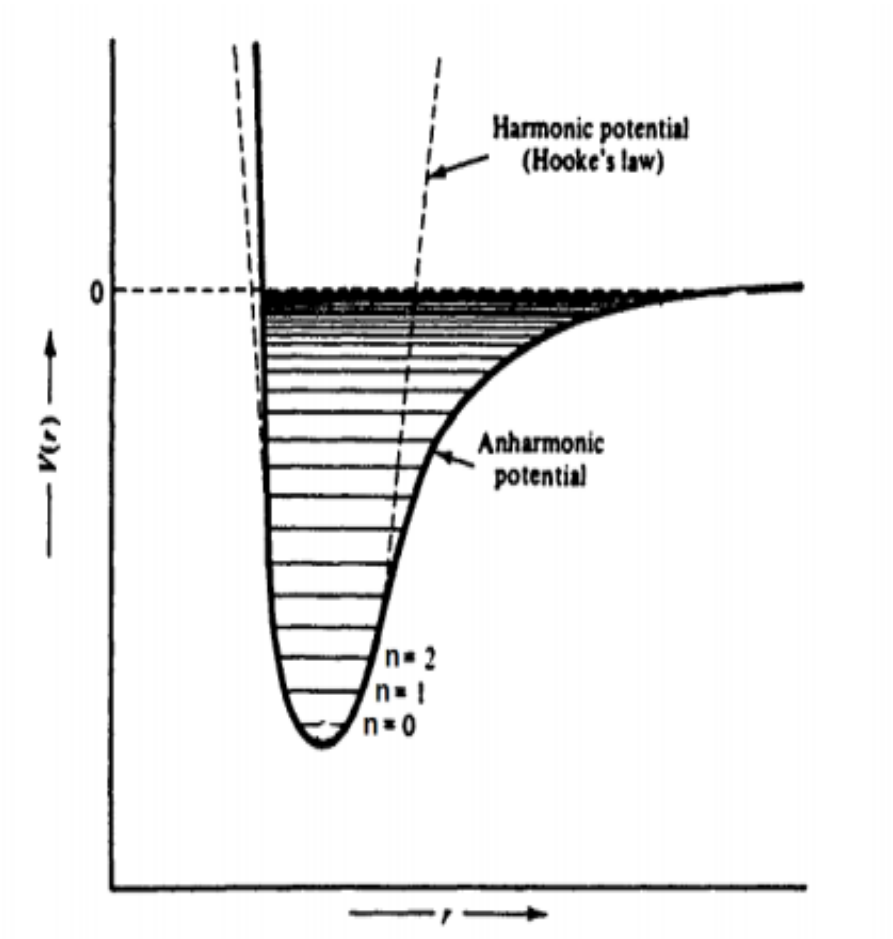

Figure2. 5: The potential energy diagram comparison of the anharmonic and the harmonic oscillator. Vibration energy states are denoted by n(Henry et al.,1968).

2.4 FT-IR Spectroscopy

Since the development of the first spectrophotometers in the beginning of 20^{th} century, a rapid technological development has taken place. The first generations of spectrometers were dispersive ones. Initially, the dispersive elements were prisms, and later, they changed over the gratings.(Kačuráková et al., 2001).

In the mid1960s IR spectroscopy witnessed a revival due to the advent of spectrometers that used the Fourier transform. The second-generation spectrometers, with an integrated Michelson interferometer, provided some significant advantages compared to dispersive spectrometer. The most important advantage of FT-IR spectroscopy for biological studies is that of almost any biological system can be obtained in a variety of environment.(Naumann et al.,1991).

2.4.1 Infrared (IR) Spectroscopy:

IR spectroscopy is certainly one of the most important analytical techniques available to today's scientist. One of the great advantages of IR spectroscopy is that its samples may be virtually studied; liquids, solution, pastes, powders, films, fibers, gases, and surface can all be examined through a judicious of sampling technique.(Siesler et al.,2008).

2.4.1.1 IR-region:

Infrared radiation spans a section of electromagnetic radiation spectrum next to the visible spectra region, and extends from wavelength, IR spectroscopes don’t usually use the wavelength to plot their spectra, but rather the inverse of wavelength; wave number; This measure has the advantage of being proportional to vibrational frequency and the vibrational energy. So, the wavenumber range of IR radiation is from about 12800 to 10

cm^{-1} .IR spectrum is conveniently divided into three regions due to their place on visible spectrum near, mid, and far-IR regions ; The rough limits of each are shown in figure (2.6).(Stuart et al., 2005).

2.4.1.2 IR Spectrum presentation:

In IR spectroscopy, the horizontal coordinate of the spectrum runs from high wavenumbers to low wavenumbers according to the recommendation of the international union of pure and applied chemistry. This is equal to running from small wavelength to large wavelength (Villringer et al.,1993).

IR absorption is generally presented in the form of a spectrum showing wavelength or wavenumber versus transmittance or absorption intensity The Transmittance (T), is the ratio of radiant power transmitted by the sample (I) to the radiant power incident on the sample (I_0) Absorbance (A) is the logarithm to the base 10 of reciprocal of the transmittance (T) as shown in equation (11).

$$A = \ell og_{10}(\frac{1}{T}) = -\ell og_{10}T = -\ell og_{10}\frac{I}{I_0} \text{ ..... } (11)$$

2.4.1.3 Theory of FT-IR Spectroscopy:

Interferometer is the heart of FTIR spectrometer. Basically, it works according to Michelson interferometer. Michelson interferometer takes a beam of light, splits it into two beams, and makes one of them travel a different distance than the other. The optical path difference δ is the difference in distance traveled by these two beams. (Griffiths et al., 2007).

Interferometer is the major component of most FTIR spectrometers, a diagram of a Michelson interferometer is shown in Figure (2-6)

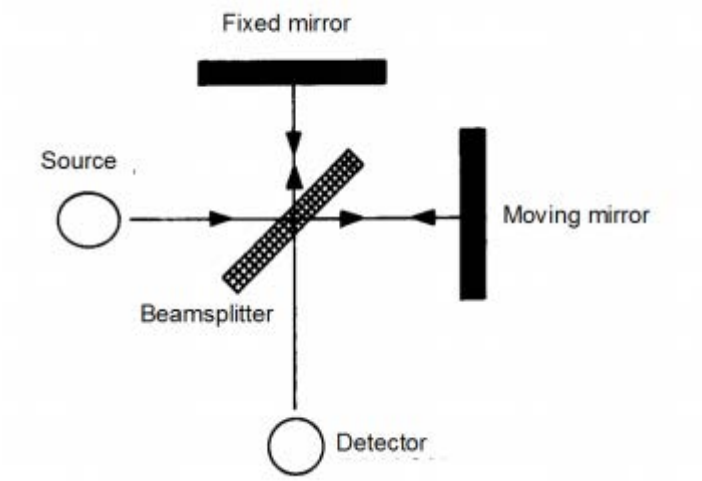

Figure2. 6: An optical diagram of Michelson interferometer. (Ferraro et al., 2012)

The beamsplitter is designed to reflect half of the radiation that falls onto it and transmits the other. The transmitted light strikes the moving mirror and the reflected light strikes the fixed mirror. After reflecting off their respective mirrors, the two light beams interfere at the beam splitter, and then leave the interferometer to the sample compartment, interact with the sample, and continue to the detector. (Ferraro et al.,2012).

Zero path difference (ZPD) occurs when the reflected and the transmitted beam travel the same distance. The mirror displacement is the distance that the mirror moves ZPD relative to(Backx et al., 1977; Ferraro et al., 2012) ,and is denoted by Δ .The relationship between mirror displacement and optical path difference is shown in equation (12).

$$(\delta = 2\Delta)\ldots\ldots\ldots \qquad (12)$$

When the recombined beams, reflected off the fixed and moving mirrors, on the beamsplitter the two beams of light interfere the result will be a light beam of double amplitude (constructive interference) if the interferometer is in ZPD(Smith et al, 2011). This constructive interference also happens at the case of equation (13).

$$(\delta = n * \lambda)\ldots\ldots\ldots \qquad (13)$$

Where n is any integer with the values n= 0, 1, 2, 3…….

A destructive interference occurs, and the amplitude for each beam cancels that of the other as can be seen in Figure 2.7 and equation (14) .

$$(n + \frac{1}{2})\lambda \ldots\ldots\ldots \qquad (14)$$

Where n is any integer with the values n= 0, 1, 2, 3….

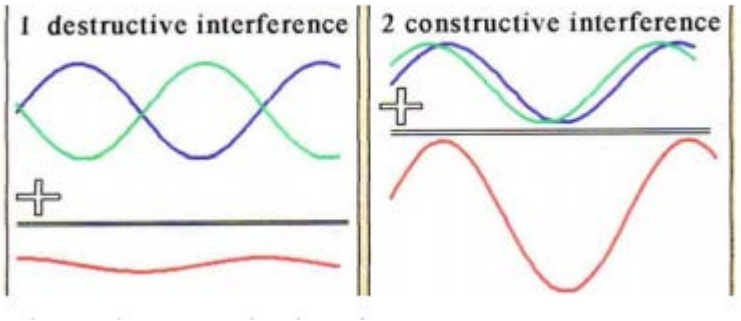

Figure2. 7: Destructive and constructive interference.(Smith et al., 2011)

A combination of constructive and destructive interference occurs, making the light beam intensity somewhere very bright and very weak light beam. It allows the interferometer goes through the sample compartment and focuses upon the detector which measures the light intensity variation with optical path difference as cosine wave interferogram is Fourier transformed to give a spectrum.(Smith et al., 2011)

Spectrum is calculated by Fourier transform of the interferogram. Ideally, the limits for Fourier transform integral should be plus and minus infinity.(Jaggi et al., 2006) The essential equations are related to the light intensity falling on detector I (t), to the spectral intensity B (ν) are equations (15) and (16).

$$I(t) = \int_{-\infty}^{+\infty} B(v)e^{-i2\Omega vt}\,dv \text{ ……..(15)} \qquad B(v) = \int_{-\infty}^{+\infty} I(t)e^{-2i\Omega vt}\,dv \text{ ……. (16)}$$

Where ν is the wavenumber

2.4.1.4 The working principe of FT-IR spectrometer:

The basic components of an FT-IR spectrometer are shown in figure (2-8). The working principle of an FT-IR spectrometer is as follow. A steady illumination from a broad band-IR source is modulated by Michelson interferometer i.e. a beam splitter that divides the collimated light along different paths to two mirrors.(Griffith et al , 1996).

The light reflected from the fixed and the moving mirror is recombined at the beam splitter and is directed through the sample and into the IR detectors. The path length difference between the light reflected from the fixed mirror and the moving mirror is measured very precisely(Kos et al.,2002). Next, the computer stores the digitized interferogram and converts it via Fourier transform to an IR spectrum(Černá et al., 2003) as described in figure (2.8).

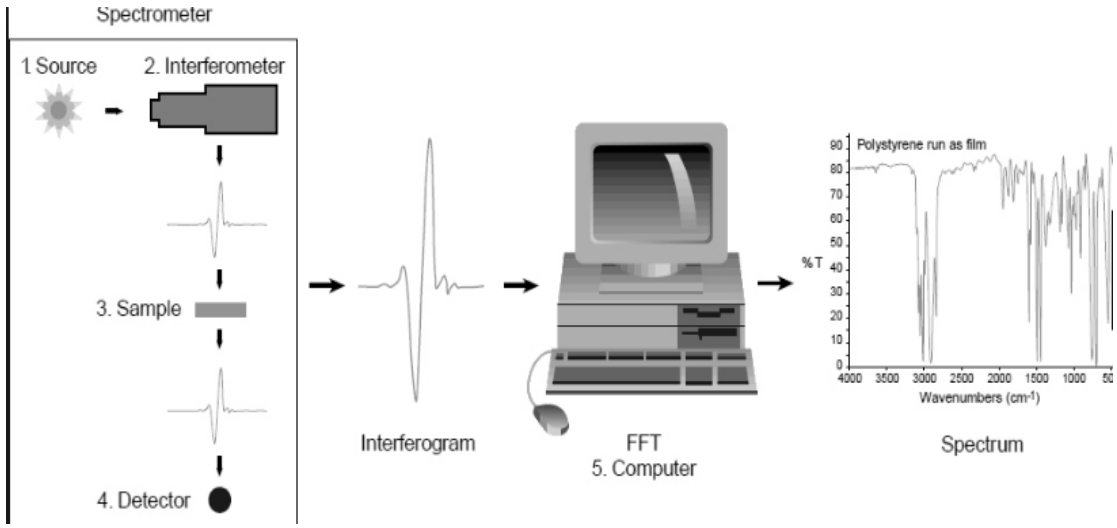

Figure2. 8: FTIR layout and basic components.(Černá et al., 2003)

2.5 Ultraviolet visible spectrophotometer

When continuous radiation passes through a transparent material, a portion of the radiation may be absorbed. In the case of UV-VIS spectrophotometer, the transitions that result in the absorption of electromagnetic radiation in this region of the spectrum are the ones between electronic energy level. As a molecule absorbs energy, an electron is promoted from an occupied orbital to an unoccupied one of a greater potential energy.(Saxena et al., 2010)

For most molecules, the lowest energy occupied molecular are orbital's which correspond to the bonds. The orbital's lie at somewhat higher energy levels. The orbitals that hold unshared pairs and nonbonding (n) orbital's lie at even higher energy(Rossel et al., 2006).

The unoccupied , or antibonding orbitals ($\pi^{*} and \sigma^{*}$) ,are the orbitals of highest energy , figure(2.9) , shows a typical progression of electronic energy levels.

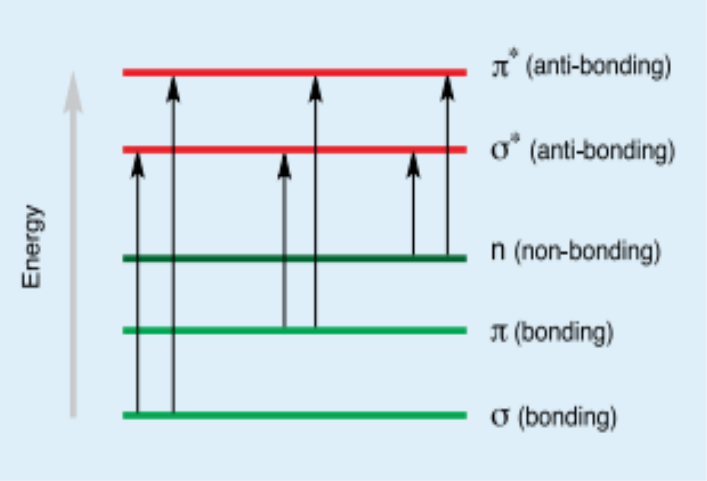

Figure2. 9:Electronic energy levels . (Rossel et al., 2006)

In all compounds , the electronic may undergo several possible transitions of different energies Figure (2.10) show these transitions.

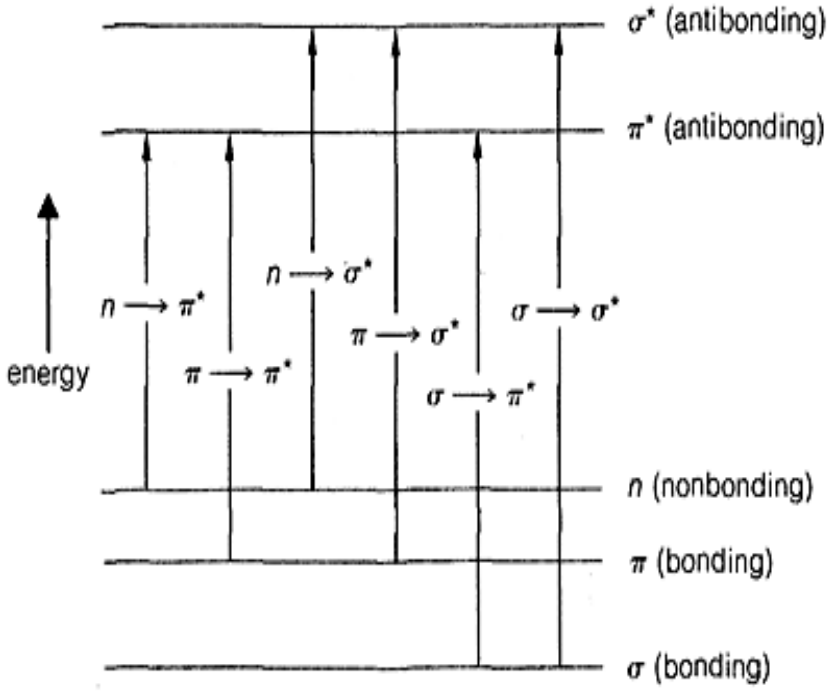

Figure2. 10:Electronic energy transitions.(Pople et al., 1970).

A spectrophotometer is an instrument that measures the intensity of the light beam. It behaves as a function of wavelength Spectrophotometers for the measurement of absorbance in the UV-VIS range coming in a variety of configurations. The most common routine laboratory instruments are single-or double –beam devices made up of light source, monochromatic, sample compartment, detectors, data processor and display.(Kamentsky et al., 1965).

The absorption of UV light by proteins has been analyzed in detail and proposed as a structural probe from the very early days of molecular biology. The absorption of proteins in the UV-VIS arises mainly from the electronic bands in the aromatic amino acid side-chains (tryptophan, tyrosine, and phenylalanine) and to less extent, cysteine residues, close to 290 nm.(Beaven et al.,1952).

2.6 Fluorescence

Fluorescence spectrophotometer is one of the most widely used spectroscopic techniques in the field of biochemistry and molecular biophysics today(Li et al., 2011). Fluorescence is a particular case of luminescence. The other case is the phosphorescence Luminescence which is an emission of ultraviolet, visible or infrared photons from an electronically excited species(Zhu et al., 2014). Fluorescence is a phenomenon whereby a material absorbs light at one wavelength and then emits it at a longer wavelength.(Eftink et al., 1981).

The processe that accur between the absorption and emission of light are usually illustrated by the Jablonski digram , a typical jablonski digram is show in figure (2-11) (Dulkeith et al., 2002) .The singlet ground , first , and second electronic states are depicted by S_0, S_1 ,and , respectively.At each of these electronic energy levels the fluorophores can exist in a number of vibrational energy levels , depicted by 0,1,2 ---- etc The transtions between states are depicted as verticallines to illustrate the instantaneous nature of light absorption.(Anger et al., 2006).

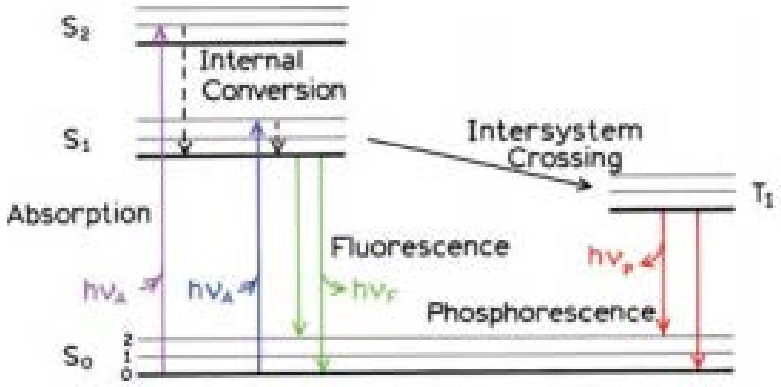

Figure2. 11: One form of a Jablonsik digram .(Genty et al., 1989)

The fluorescence lifetime and quantum yield are the most important characteristics of a fluorophore. Quantum yield is the amount of the emitted photons related to the number of the absorbed photons. The lifetime determines the time available for the fluorophore to interact with or diffuse in its environment, and then the information available from its emission(Magde et al., 2002).

Following light absorption, several processes usually occur. A fluorophore is usually excited to some higher vibrational level of either S_1 or S_2 .An interesting consequence of emission to higher vibrational ground states is that the emission spectrum is typically a mirror image of the absorption spectrum of the $S_0 \rightarrow S_1$ transition (Morris et al.,1976). This similarity occurs because electronic excitation does not greatly alter the nuclear geometry. Hence the spacing of the vibrational energy levels of the excited states is similar to that of the ground state. As a result, the vibrational structures seen in the absorption and the emission spectra are similar.(Strickler et al., 1962).

Upon excitation into higher electronic and vibrational levels, the excess energy is quickly dissipated, leaving the fluorophore in the lowest vibrational level of S1. This relaxation occurs in about 10–12 s and is presumably a result of a strong overlap among numerous states of nearly equal energy. Because of this rapid relaxation, emission spectra are usually independent of the excitation wavelength(Najbar et al., 1991).

The intensity of fluorescence can be decreased by a wide variety of processes. This decrease in intensity is called quenching. Quenching can occur by different mechanisms. Collisional quenching occurs when the excited-state fluorophore is deactivated upon contact with some other molecule in solution, which is called the quencher(Boens et al., 2007).

For collisional quenching the decrease in intensity is described by the well-known Stern-Volmer equation as described in equation (17).

$$\frac{F_0}{F} = 1 + K_q \tau_0 (\ell) = 1 + k_{sv} (\ell) \quad \text{.....(17)}$$

In this expression k_{sv} is the Stern-Volmer quenching constant, k_q is the bimolecular quenching constant, τ_0 is the unquenched lifetime, and ℓ is the quencher concentration. The Stern-Volmer quenching constant k_{sv} indicates the sensitivity of the fluorophore to a quencher. In protein ,Tryptophan , PhenyPhenylalanine, and Tyrosine ; are the amino-acid reidues that are responsible for the energy absorption and emission.

2.7 Proteins

A protein is an organic compound has carbon, hydrogen, oxygen, nitrogen, and sometimes sulfur. A protein is made up of small molecules called amino acids as shown in figure (2.12). There are 20 different amino acids commonly found in the proteins of living things which have the same basic structure (the amine group (NH2),central carbon atom (alpha-carbon) and a carboxyl group (COOH)) .The difference between one protein and another is on the side chain (labeled R in the figure below)(Palau et al.,1982).

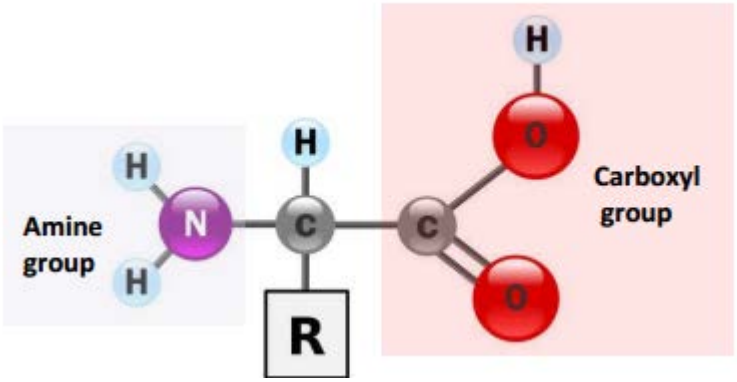

Figure2. 12: General structure of all amino acids. Only the side chain, R, varies from one amino acid to another. Variable side chains give amino acids different chemical properties(Palau et al., 1982)

Amino acids bind together through covalent peptide bonds as shown in figure (2.13); they form a long chain called a polypeptide. Polypeptides have as few as 40 amino acids or as many as several thousand. Protein consists of one or more polypeptide chains. Sequence of amino acids in a protein's polypeptide chain(s) determines the overall structure and chemical properties of the protein.(Surewicz et al., 1988).

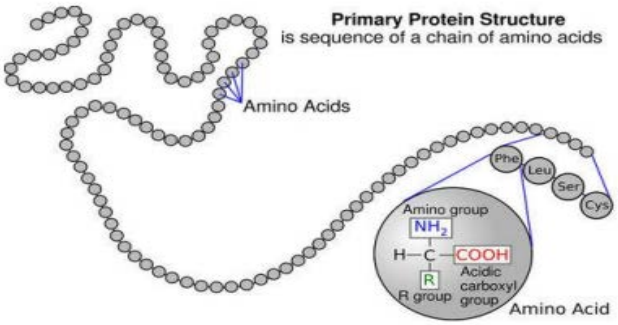

Figure2. 13:Primary protein structure.(Conte et al., 1999)

Four levels of protein structure determine its four functions: the primary, the secondary, the tertiary, and the quaternary. The primary is the simplest level of protein structure and has a sequence of amino acids in a polypeptide chain. It's unique for each protein(Conte et al., 1999).Local folded structures that are formed within a polypeptide, due to the interactions between the carbonyl O of one amino acid and H of another one, is a secondary structure see figure (2.14). Its most common types are the α helix and the β pleated sheet. α helix and the β pleated sheet structures are held in shape by hydrogen bonds(Janin et al., 1990).

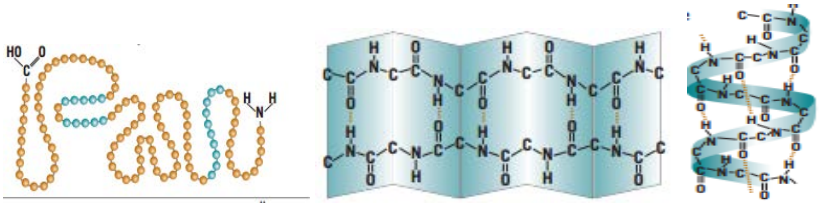

Figure2. 14: Primary structure of protein, Beta sheet and α helix respectively(Surewicz et al ., 1988)

Tertiary structure is three-dimensional spaces see figure (2.15). It's formed as a result of interactions between the amino acids R groups. The interaction includes hydrogen bonding, ionic bonding, dipole-dipole interactions, and London dispersion forces. Proteins are made up of multiple polypeptide chains known as subunits. When subunits come together, they give protein its quaternary structure, such as hemoglobin and DNA polymerase.(Palau et al., 1982)

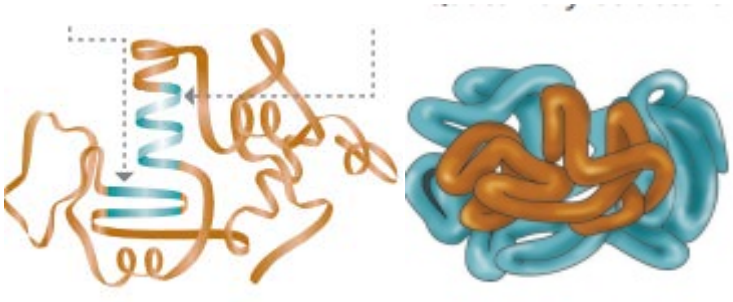

Figure2. 15: Tertiary and quaternary structure of protein respectively.(Janin et al., 2000)

2.7.1 Human Serum Albumin:

Albumin is the major soluble protein constituent of the circulatory system. Albumin has important functions in many fields of science such as pharmaceutical science, medical science, biology and chemistry, this functions are related to the fixation and transport of numerous metabolites, hormones, endogenous and exogenous substances (e.g. pharmaceutical drugs, fatty acids, etc.…).(Carter et al., 1994). Albumin is a carrier of many drugs to different molecular targets.(Sudlow et al.,1976).

Drugs binding and displacement reactions with serum albumins are important determinant of drug pharmacokinetics, restricting the unbound concentration, affecting drug distribution and elimination(Gillian et al.,1975).The general structure of albumin is characterized by several long α (alpha) helices, which allows it to maintain a relatively static shape.(Petitpas et al., 2001).

Human serum Albumins (HSA) are the most abundant and prominent plasma proteins in mammals (about 60% of the total protein. HSA concentration in blood plasma is ($40\frac{mg}{mI}$).

It also has a molecular mass of about 65 KDa and comprises 585 amino acid residues and it's synthesized in the liver. (Yamasaki et al., 1996).

HSA is soluble, a single and non-glycosylated polypeptide that is organized to form a heart-shaped protein with about 67% α-helix as its basic structure. It's a single polypeptide that is composed of three homologous domains (I-III) connected by flexible hinge region that forms a heart-shaped structure in aqueous solution. Each domain has two sub-domains (A and B) which have common structural motifs by various forces such as salt bridges and hydrophobic interactions.(Sugio et al., 1999).

HSA is a tertiary structure at 2.5 Å resolutions. Its complete three–dimensional structure has recently been determined by X-ray crystallography, and the binding sites for several drugs were also localized as seen in Figure(2-16)(Abou-Zied et al., 2008):

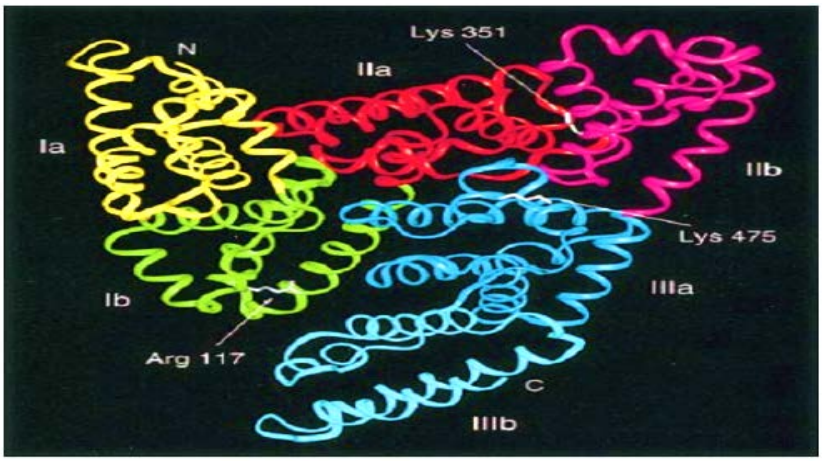

Figure2. 16: Schematic drawing of the HSA molecule. Each sub domain is marked with a different color (Abou-Zied et al., 2008)

Investigation of the binding interaction between drugs and serum albumin is very important in pharmacology and pharmacodynamics. Distribution of drugs is controlled by HSA. Because most drugs that travel in plasma bind to the sites, hydrophobic compounds will not freely dissolve in the bloodstream. The abundance and flexibility of human serum albumin allow these molecules to bind to it and carried in the bloodstream throughout the body.(He et al., 1992) .

The drug binding and displacement reactions with HSA strongly influence the distribution, the elimination and the pharmacological effect of the drug. The binding process affects drug movement into tissues and the compound's therapeutic efficacy, toxicity, and pharmacokinetics.(Bhattacharya et al., 2000) .HSA is capable of binding reversibly a variety of drugs, resulting in an increased solubility in plasma, decreased toxicity, and/or protection against oxidation of the bound ligand.(Zsila et al., 2003).

The protein's ability of binding aromatic and heterocyclic compounds largely depends on the existence of two major binding regions, namely Sudlow, s sites I and II. Site I is known as the warfarin binding site. It is formed by a pocket in subdomain IIA and contains the only tryptophan of HSA (Trp 214). Site II is located in subdomain IIIA and is known as the benzodiazepine binding site as shown in figure (2.17).(Kragh et al., 1990).

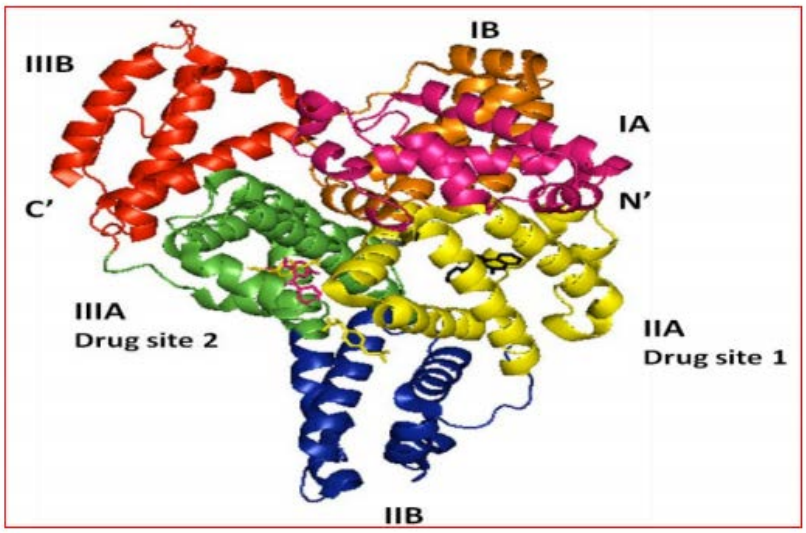

Figure2. 17: The drugs binding sites determined on the HSA structure.(He et al.,1992)

Bulky heterocyclic anions bind to site I (located in subdomain IIA), whereas site II (located in subdomain IIIA) is preferred by aromatic carboxylates with an extended conformation.(He et al , 1992)

Chapter Three: Experimental Part

This section consists of three parts, the first one includes information about the sample that I used and thin film preparation, the second one contains a full description about the spectroscopic techniques that I used in this work, which are (Bruker IFS 66/S FT-IR spectrophotometer), UV-VIS spectrophotometer (NanoDropND-1000), and Fluorospectrometer (Nano Drop 3300).

The final section presents the experimental procedure in details.

Rules for Solutions prepration

When we preparing any solution, we must place the solid (solute) first then add the liquid which is the solvent (buffer) to reach the indicated mark as shown in below figure . We can't add the solute to the solvent otherwise the final volume will be a little larger than what is supposed to be which means the final molarities will be different.

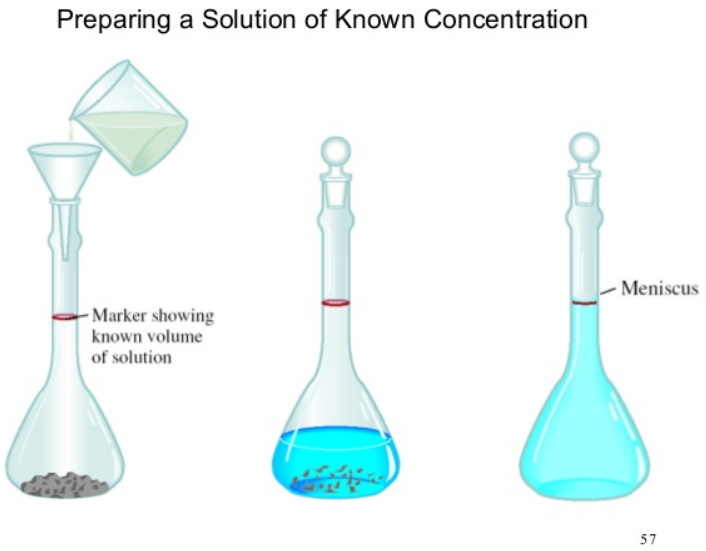

3.1 Samples and materials

HSA protein, Procaine, and Dopamine in powder form were purchased from Sigma Aldrich chemical company and they were used without further purifications. The data were collected using samples in two forms, the first one in thin film form for FT-IR technique and the second one in liquid form for both UV-VIS and fluorescence measurements**.**

3.1.1 UV-VIS and FLU Techniques:

3.1.1.1 Preparation of HSA Stock Solution:

HSA protein was prepared in a concentration of [1.2mM] as stock one by dissolved [0.08g] of protein in [1mL] phosphate buffer saline PH (7.4), in order to get a final concentration of [0.6mM] in final Drug-HSA complex solution .

3.1.1.2 Preparation of HSA final concentration :

HSA protein solution with animal concentration of [40mg/mL] was prepared by dissolved [0.04 g] of protein in powder form in [1mL] buffer saline.

3.1.1.3 Prepration of Procaine stock solutions:

Procaine with molecular weight of (272.28 g/mole) and morality of [4.8mM] were prepared by dissolved [0.0131 gram] of procaine in [10ml] volumetric flask of buffer saline PH (7.4) , then it's used to prepare different concentrations of procaine drug using dilution equation as shown in equation (3.1) and table (3.1):

$$M_1 \times V_1 = M_2 \times V_2 \ldots\ldots\ldots (1)$$

Table3. 1: Procaine Standard Solutions.

Pro initial	Pro Final	
4.8 mM stock	3.6	I took [0.75ml] from the stock Pro and place it in [1ml] Volumetric flask. Fill to the mark with saline (bottom of meniscus)
3.6	2.4	I took [0.67ml] from the 3.6 mM and place it in 1 ml volumetric flask Fill to the mark with saline
2.4	2.0	I took [0.83ml] from the 2.4 mM and place it in 1 ml volumetric flask Fill to the mark with saline
2.0	1.2	I took [0.6ml] from the 2.0 mM and place it in 1 ml volumetric flask Fill to the mark with saline
1.2	1	I took [0.83ml] from the 1.2 mM and place it in 1 ml] volumetric flask Fill to the mark with saline
1.0	0.8	Take [0.8ml] from the 1.0 mM and place it in 1 ml volumetric flask Fill to the mark with saline
0.8	0.6	Take [0.75ml] from the 0.8 mM and place it in 1ml volumetric flask Fill to the mark with saline
0.6	0.3	Take [0.5ml] from the 0.6 mM and place it in 1ml volumetric flask Fill to the mark with saline

3.1.1. 4 Preparation of Procaine –HSA complex solutions:

To prepare the complexes, we kept HSA as close as possible to 0.6 mM (the concentration in plasma). Mix [50 μl of the HSA stock + 50 μl of each of the Pro standards sol'n] the molarities of them will be halved to be as described in table 3.2:

Table3. 2: preparing Pro-HSA complexes.

Pro sol'n (mM)	HSA stock (mM)	Volume HSA stock	Volume Pro Soln	Final total volume	Final HSA (mM)	Final Pro (mM)	[Pro]/[HSA]
4.8	1.2	50 μl	50 μl	100 μl	0.6	2.4	2.4/0.6 = 4.0
3.6	1.2	50 μl	50 μl	100 μl	0.6	1.8	1.8/0.6 = 3.0
2.4	1.2	50 μl	50 μl	100 μl	0.6	1.2	1.2/0.6 = 2.0
2.0	1.2	50 μl	50 μl	100 μl	0.6	1.0	1.0/0.6 =1.67
1.2	1.2	50 μl	50 μl	100 μl	0.6	0.6	0.6/0.6 = 1.0
1.0	1.2	50 μl	50 μl	100 μl	0.6	0.5	0.5/0.6 = 0.83
0.8	1.2	50 μl	50 μl	100 μl	0.6	0.4	0.4/ 0.6=0.67
0.6	1.2	50 μl	50 μl	100 μl	0.6	0.3	0.3/ 0.6 = 0.5
0.3	1.2	50 μl	50 μl	100 μl	0.6	0.15	0.15/0.6=0.25

3.1.1.5 Preparation of Dopamine Stock Solution:

Dopamine with molecular weight of [189.2g/mole] and molarity of [4.8mM] were prepared by dissolved [0.0091g] of dopamine in [10ml] volumetric flask of buffer saline PH (7.4)as stock solution then it used to prepare different concentrations of DA using dilution equation as Pro drug, see equation (2) and table 1.2

$$M_1 \times V_1 = M_2 \times V_2 \quad \text{.....(2)}$$

Table3. 3: Dopamine Standard Solutions.

DA initial	DA Final	
4.8 mM stock	3.6	I took [0.75ml] from the stock DA and place it in [1ml] Volumetric flask. Fill to the mark with saline (bottom of meniscus)
3.6	2.4	I took [0.67ml] from the 3.6 mM and place it in 1 ml volumetric flask Fill to the mark with saline
2.4	2.0	I took [0.83ml] from the 2.4 mM and place it in 1 ml volumetric flask Fill to the mark with saline
2.0	1.2	I took [0.6ml] from the 2.0 mM and place it in 1 ml volumetric flask Fill to the mark with saline
1.2	1	I took [0.83ml] from the 1.2 mM and place it in 1 ml] volumetric flask Fill to the mark with saline
1	0.8	Take [0.8ml] from the 1.0 mM and place it in 1 mL volumetric flask Fill to the mark with saline
0.8	0.6	Take [0.75ml] from the 0.8 mM and place it in 1mL volumetric flask Fill to the mark with saline
0.6	0.3	Take [0.5ml] from the 0.6 mM and place it in 1mL volumetric flask Fill to the mark with saline

3.1.1.6 Preparation of Dopamine –HSA complex solutions:

To prepare the complexes, we kept HSA as close as possible to 0.6 mM (the concentration in plasma). Mix [50 μl of the HSA stock + 50 μl of each of the DA standards sol'n] the molarities of them will be halved to be as described in table 3.4:

Table3. 4: Preparing of DA-HSA complexes.

DA sol'n (mM)	HSA stock (mM)	Volume HSA stock	Volume DA Soln	Final total volume	Final HSA (mM)	Final DA (mM)	[DA]/[HSA]
4.8	1.2	50 μl	50 μl	100 μl	0.6	2.4	2.4/0.6 = 4.0
3.6	1.2	50 μl	50 μl	100 μl	0.6	1.8	1.8/0.6 = 3.0
2.4	1.2	50 μl	50 μl	100 μl	0.6	1.2	1.2/0.6 = 2.0
2.0	1.2	50 μl	50 μl	100 μl	0.6	1.0	1.0/0.6 = 1.67
1.2	1.2	50 μl	50 μl	100 μl	0.6	0.6	0.6/0.6 = 1.0
1.0	1.2	50 μl	50 μl	100 μl	0.6	0.5	0.5/0.6 = 0.83
0.8	1.2	50 μl	50 μl	100 μl	0.6	0.4	0.4/ 0.6 = 0.67
0.6	1.2	50 μl	50 μl	100 μl	0.6	0.3	0.3/ 0.6 = 0.5
0.3	1.2	50 μl	50 μl	100 μl	0.6	0.15	0.15/0.6= 0.25

3.1.2 FT-IR Technique:

HSA stock solution [1.2mM] , final one [0.6mM] , DA and Pro drugs complexes for IR spectroscopic technique also prepared in such way of UV-VIS and fluorescence technique as described in tables [3.1, 3.2, 3.3, and 3.4]

3.1.2.1 Thin film preparation:

Silicon windows (NICODOM Ltd) were used as spectroscopic cell windows, 60µl of each sample of HSA-procaine complex solution and Dopamine-HSA complex solution was spread on silicon window using spincoater to get homogenous thickness for all samples as possible as I could, then incubator was used to evaporate the solvent in order to obtain transparent thin film on the silicon window. All solutions were prepared at the same time at room temperature and they stored at same conditions.

3.2 Instruments

Many instruments can be used to study the interaction between HSA and the drugs. In this work the following instruments have been used to take the data.

3.2.1 FT-IR spectrometer:

FT-IR measurements were obtained used Bruker IFS 66/S spectrophotometer equipped with a liquid nitrogen-cooled MCT detector and KBr beam splitter**.** Data were analyzed using Bruker IFS 66/S software and origin program**.**

3.2.2 UV-VIS spectrophotometer (Nano Drop ND-1000):

The absorption spectra for HSA with two drugs were obtained by using of Nano Drop ND-1000 Spectrophotometer at Nanotechnology Lab**.** Spectrophotometer used to measure the absorption spectrum of protein and two drugs complex solution in the range between **220 - 750**nm with high accuracy**.**

3.2.3 Fluorospectrometer (NanoDrop 3300):

Fluorescence measurements were obtained using NanoDrop ND-3300 Fluorospectrophotometer at Nano technology lab, the excitation source of this instrument is one of three solid state lights emitting diode (LED). UV-LED with maximum excitation of (365) nm. Blue-LED with maximum excitation of (470nm), and white LED which has a range of excitation between (500-650nm).

Many instruments also used in this work such as spincoater to make the thin films sample homogenous as possible as we can also digital balance, vortex, and Micropipettes.

3.3 Expermental Procedure

3.3.1 UV-VIS Spectrophotometer experimental procedure:

The procedure of UV-VIS spectrophotometer which used in this work was described in Nano Drop 1000 spectrophotometer (V3.7, 2008, User's manual, Nano Drop 1000 spectrophotometer 3.7, User manual, 2008) as follows:

Operation

1 μl sample of Procaine and Dopamine was pipette into the end of a fiber optic cable (the receiving fiber). A second fiber optic cable (the source fiber) is then brought into contact with the liquid sample causing the liquid to bridge the gap between the fiber optic ends.

The gap is controlled to both 1mm and 0.2 mm paths. A pulsed xenon flash lamp provides the light source and a spectrometer utilizing a linear CCD array is used to analyze the light after passing through the sample. The instrument is controlled by PC based software, and the data is logged in an archive file on the PC.

Basic Use: The main step for using UV-VIS spectrophotometer is described in (NanoDrop 1000 Spectrophotometer 3.7, user manual 2008) as follows:

1. Open the sample arm then pipette the sample of Procaine or Dopamine onto the lower measurement pedestal as described on the first photo of fig (3.1**).**

2. Close the sampling arm and initiate a spectral measurement using the operating software on the PC. The sample column is automatically drawn between the upper and lower measurement pedestals and the spectral measurement made; see the second photo of fig (3.1).

3. When the measurement is complete, open the sampling arm and wipe the sample from both the upper and lower pedestals using a soft laboratory wipe. Simple wiping prevents

sample carryover in successive measurements for samples varying by more than 1000 fold in concentration see the last photo of figure (3.1)(Scientific, 2009).

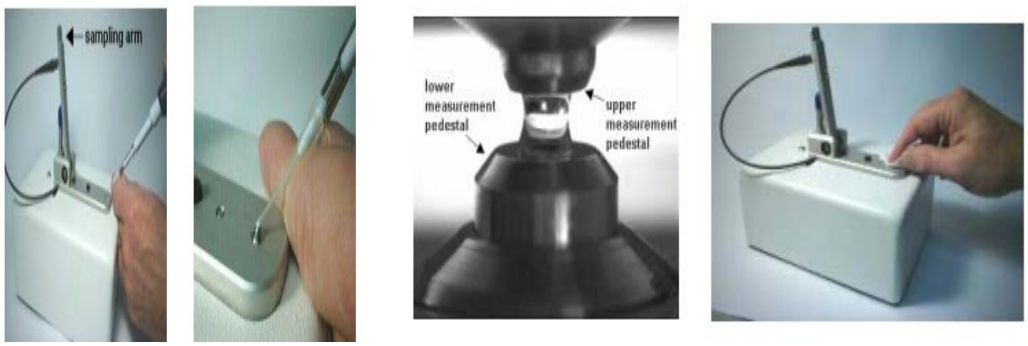

Figure3. 1: Main steps for using the sample UV-VIS Spectrophotometer . (Scientific, 2009)

3.3.2 Fluorospectrophotometer experimental procedures:

The experimental procedure of fluorospectrophotometer was described in details in (Nano Drop 3300 fluorospectrophotometer V3.7 user manual, 2008) as follows:

Operation

1-2 μl sample of Procaine or Dopamine is pipette onto the end of the lower measurement pedestal (the receiving fiber). A non-reflective "bushing" attached to the arm is then brought into contact with the liquid sample causing the liquid to bridge the gap between it and the receiving fiber.

The gap or path length is controlled to 1mm. Following excitation with one of the three LEDs, emitted light from the sample passing through the receiving fiber is captured by the spectrometer. Nano Drop 3300 is controlled by software run from a PC. All data is logged and archived in the C:\ND-3300 Data folder as well as at a second user defined location.

Basic Use:

The main steps for making a measurement are listed below as described in (NanoDrop 3300 spectrophotometer V3.7 user manual, 2008) and the photos show it clearly.

1. With the sampling arm open, pipette the sample of Procaine or Dopamine onto the lower measurement pedestal see the first photo of fig (3.2).

2. Close the sampling arm and initiate a measurement using the operating software on the PC. The sample column is automatically drawn between the upper bushing and the lower measurement pedestal and the measurement is made, see the second photo of fig (3.2).

3. When the measurement is complete, open the sampling arm and blot the sample from both the upper bushing and the lower pedestal using low lint laboratory wipe, see the last photo of figure (3.2).

Figure3. 2: Main steps for using the sample flurospectrophotometer (Nano Drop 3300 fluorospectrophotometer V3.7 user manual, 2008)

3.3.3 FT-IR Spectrometer experimental procedures:

The absorption spectra of HSA with drugs were obtained in the range of (400-4000) cm^{-1} these spectra were taken as an average of 65 scans**.** Fourier Self –deconvolution, Baseline correction, peak picking, and normalization were applied for all spectra by OPUS software, the peak positions were determined by peak picking after we applied the deconvolution for 6 times for each spectrum since we found that this time is the best to give us the best information about the secondary structures.

IR-Spectra for HSA ,Dopamine-HSA complexes ,and Procaine –HSA complexes were obtained in the range of (1200-1800) cm^{-1}, we divides it into three amides(1700-1600) cm^{-1} represent amide I,(1600-1480) cm^{-1} represent amide II and (1330-1220) cm^{-1} represents amide III

3.3.4 FT-IR data processing:

Analysis of IR spectra in term of protein structure is not straightforward and required much technique to help with both quantitative and qualitative interpretation of spectra; in this work many data processing tasks were used.

3.3.4.1 Baseline correction:

Using baseline correction processing data, the baseline of the resultant spectra be flat line on zero, on other word there no signal. Baseline correction processing data is applied in two steps. Recognize the baseline which can be done by selecting a point from spectral points on the spectrum then adding or subtracting an intensity value from the point or points to correct baseline offset. Baseline corrections done automatically using Opus User Software (OPUS). (Lei et al., 2010)

3.3.4.2 Peak picking:

Processing data used to find the position of the peak for the spectra**.** Automated process applied in two steps, recognition of peaks, and determination of the wavenumbers values of maximum or minimum absorbance. (Lei et al., 2010) .

Before applying peak picking process for spectra, the deconvolution for six times must be applied.

3.3.4.3 Second derivative:

Second derivative used to resolve and analyze the complex protein spectrum in the range of near infrared region by separating the overlapping bands. Second derivative is used in many of quantitative and qualitative determination of protein. (Balestrieri et al.,1978)

3.3.4.4 Fourier Self Deconvolution:

Processing data to resolve overlapping of bands for spectra that have narrow bands to distinguish the spectral features. Fourier Self deconvolution applied using several steps, computation of an interferogram of the sample by computing the inverse Fourier-transform of the spectrum, and multiplication of the interferogram by a smoothing function and by a function consisting of a Gaussian–Lorentzian band shape, and Fourier transformation of the modified interferogram (Abdul-Fattah et al., 2007).

In order to get the best results in this work the deconvolution has been applied six times

Fourier self-deconvolution technique has been successfully applied in both quantitative and qualitative study of large number of protein it's give information about the change in secondary structure of that protein and also it useful for giving information of change according to other factor such as temperature, PH, ligand binding and others. (Kauppinen et al., 1981)

3.3.4.5 Spectral subtraction:

Straight forward process for analysis of complex spectra, approach that is very useful for investigating subtle differences in protein structure**.** Spectral subtraction basic principle is the subtraction of a protein absorbance spectrum in state A from that of the protein in state B, the resultant spectra of this process only shows peaks that are associated with those groups involved in the conformational change. (Martin et al , 1994).

Chapter Four: Results and Discussion

This chapter includes the main results analysis and discussions of our data. The first section includes the results that obtained from the UV-VIS spectrophotometer and we discussed it in details in that section, the second one deals with fluorescence spectrophotometer data and results, in the final section FT-IR graphs and data analysis are given**.**

4.1 UV-VIS technique

The interaction between protein and drugs plays important role and factor for both pharmacokinetics and pharmodynamics, so many researches had studied the interaction between that protein and drugs, UV-VIS spectroscopy was one of effective method used to investigate that interaction because of its high sensitivity, rapidity, and ease of implementation.(Rasoulzadeh et al., 2010 ,Suryawanshi et al., 2016)

The absorption spectra of different concentration of procaine and dopamine with fixed concentration of HSA are displayed in figure (4.1)and figure (4.2), respectively, the excitation has been done on 210 nm on other hand the absorption was done on 280 nm. It's shown from the figures that as the concentration of procaine and dopamine increased the UV intensity of HSA increases, this increment and change of absorbance can be determined as an indicator of interaction occurred between HSA protein and two drugs.

We repeated the measurements for all samples many times and it was clearly that there is no change of the consistent of the results and no significant differences were observed.

The absorbance spectra of HSA-Procaine complex have been drawn using origin software program as shown in figure (4.1).

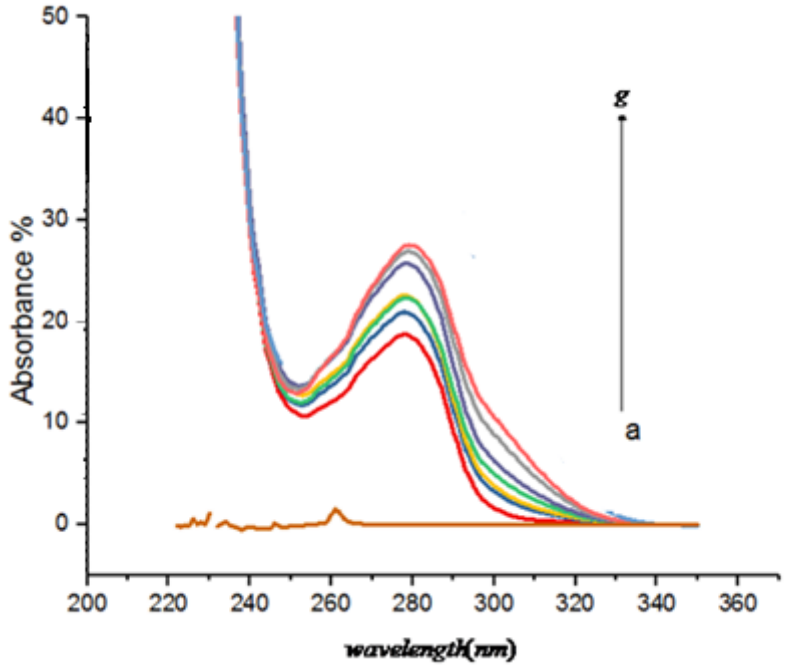

Figure4. 1: UV-Absorbance spectra of Procaine-HSA complexes at these concentration (a= Free Procaine, b= Free HSA, c=0.3 mM, d=0.4-mM, e=0.5 mM,f=0.6 mM, g=1 mM, h=1.2 mM).

HSA –DA complex spectra for different concentration of DA has been drawn using origin software as shown in figure (4-2).

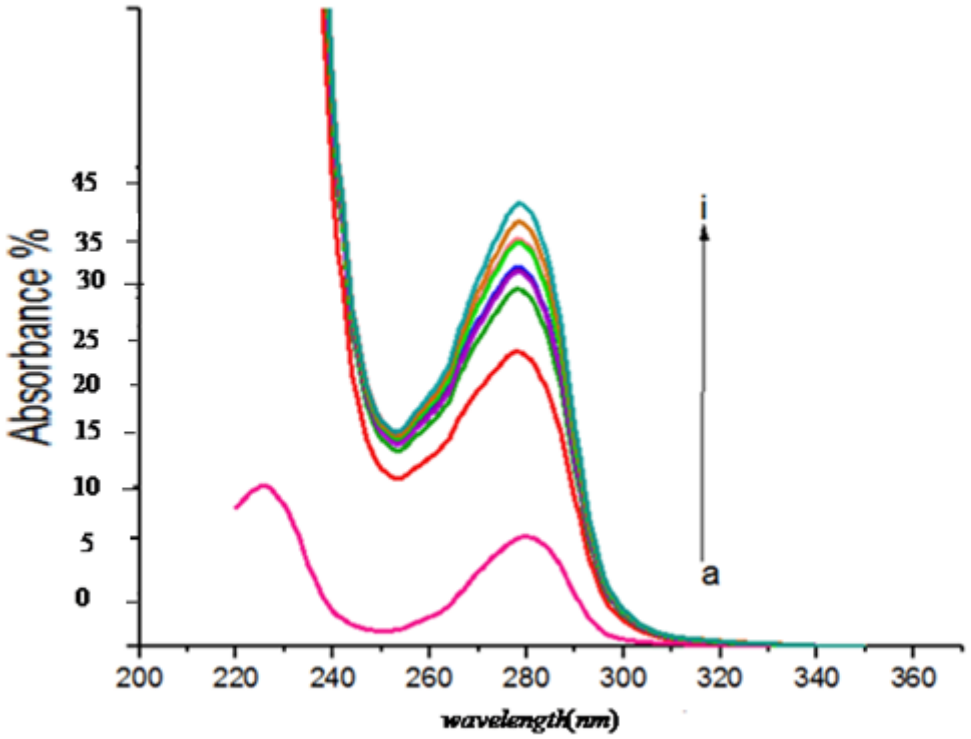

Figure4. 2: UV-Absorbance spectra of Dopamine-HSA complexes at these concentrations (a= Free DA 2.4mM, b= HSA Free, c= 0.3 mM, d= 0.4mM, e=0.5 mM, f=0.6 mM, g=1mM, h=1.2mM, i=2.4mM).

4.1.1 Binding constants of procaine, Dopamine and HSA complexes using UV-VIS technique:

(Procaine or dopamine)-HSA complexes binding constant were determined using UV-VIS spectrophotometer results according to published method (Stephanos et al., 1996), by assuming that there is only one type of interaction between procaine or dopamine and HSA in aqueous solution, which leads to establish equations (1) and (2) as follows.

HSA +Procaine $\leftrightarrow$ Procaine +HSA ……. (1)

HSA+Dopamine $\leftrightarrow$ Dopamine +HSA

K = [Procaine: HSA] / [Procaine] [HSA] …… (2)

K = [Dopamine: HSA] / [Dopamine] [HSA]

The absorption data were treated using linear double reciprocal plots based on the following equation (Marty et al., 2009).

$$\frac{1}{A - A_0} = \frac{1}{A_\infty - A_0} + \frac{1}{k(A_\infty - A_0)} \times \frac{1}{\ell} \quad \text{……. (3)}$$

Where A_0 corresponds to the initial absorption of protein at 280nm in the absence of ligand, A∞ is the final absorption of the ligand protein, and A is the recorded absorption at different procaine or dopamine concentration (L).

4.1.1.1Procaine binding constant:

Binding constant calculations of procaine were determined using equation (3) as described in table (4.1):

Table4. 1: Binding constant calculations for Procaine-HAS complexes.

Sample[mM]	Absorbance (A)	A-A0	1/(A-A0)	$(1/ L) \times 10^{+3}$ {L/mole}
b- Free HSA	18.36 [A0]	---------	----------	----------
c-0.30	20.68	2.32	0.30	3.00
d-0.40	22.00	4.00	0.25	2.50
e-0.50	23.00	4.60	0 .20	2.00
f-0.60	25.00	6.40	0.14	1.60
g-1.00	26.00	7.64	0 .12	1.00
h-1.20	27.00	8.64	0.11	0 .80

Using linear regression software program, the double reciprocal plot of 1/ (A- A_0)V_s (1/L) has been fitted to get the best linear curve as shown in figure (4.3).

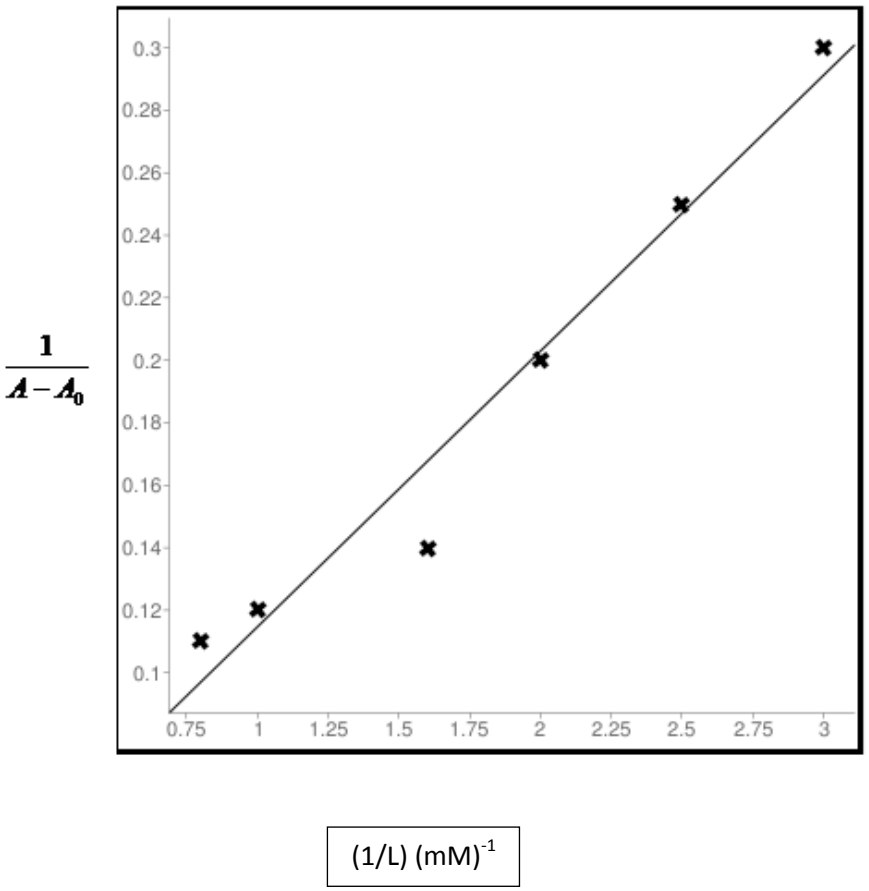

Figure4. 3: The plot of 1/ (A-A_0) vs. 1/L for HSA with different concentration of procaine

linear fitting for the points of HSA-Procaine complex has been found to be as described in next equation:

$$Y=0.0801786+0.080020267x$$

Intercept = 0.0801786 Slope = $0.080020267 \times 10^{-3}$

Using last equation binding constant (K) can be estimated from the ratio of the intercept to the slope to be [1.00115599×10^3] for procaine –HSA complexes.

The value obtained is indicative of a weak procaine protein interaction with respect to other drug-HSA complexes with the binding constant in the range of 10^5 and $10^7 M^{-1}$ (Zhong, 2004).

4.1.1.2 DA binding constant:

Binding constant calculations of Dopamine were determined using equation (3) as described in table (4.2) :

Table4. 2: Binding constant calculations for DA-HSA complex.

Sample $\times 10^{-3}$ [mole / L]	Absorbance (A)	A-A0	1/(A-A0)	1/ L$\times 10^{+3}$ {L/mole}
b- Free HSA	23.014 [A0]	--------	----------	----------
c-0.30	28.89	5.88	0.17	3.33
d-0.40	30.15	7.14	0.14	2.50
e-0.50	31.34	8.33	0 .12	2.00
f-0.60	33.01	10.00	0.10	1.66
g-1.00	35.83	12.82	0 .08	1.00
h-1.2	37.29	14.28	0.07	0.83
i-2.4	43.01	20.00	0.05	0.42

The double reciprocal plot of 1/ (A- A_0)V_s (1/L) has been obtained using linear regression software program to get the best linear line as shown in figure (4.4).

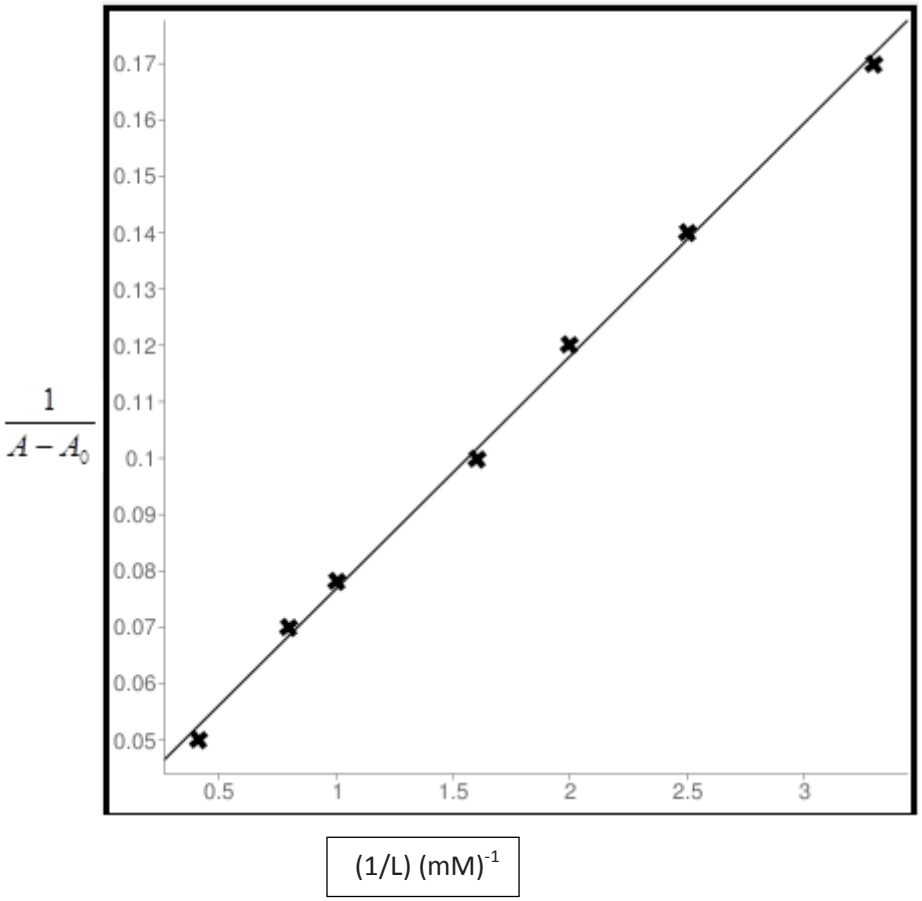

Figure4. 4: The plot of 1/ (A-A_0) vs. 1/L for HSA with different concentration of Dopamine

Linear equation of last reciprocal plot has been determined using linear regression program to be as described in the next equation.

$$Y=0.034956 +0.0411710x$$

Intercept = 0.034956 Slope= 0.0411710×10^{-3}

The binding constant (K) can be estimated from the ratio of the intercept to the slope to be (0.849044×10^{3}) for Dopamine –HSA complexes

Binding constant value of DA is indicative of a weak Dopamine protein interaction with respect to other drug-HSA complexes with the binding constant in the range of 10^{5} and $10^{7}\,M^{-1}$ (Zhong et al., 2004)

4.2 Fluorescence spectroscopy

Investigation of the binding mode between the proteins and drug has been attracted the interest of research for many years because it's extremely important to understand biopharmceutics, pharmacokinetics and toxicity of the drug as well as the relationship of structure and function of the protein. (Cheng et al., 2017)

Fluorescence absorption spectroscopy is a powerful tool for studding the interaction between the drugs and HSA protein, many drugs are not fluorescent but proteins have a fluorescent character that results from the protein's tryptophan and tyrosine residues so the auto fluorescence of HSA is originated from Tryptophan (Trp), Tyrosine (Tyr) residues.(Cheng et al., 2017 , Sułkowska et al., 2002 , Maltas et al., 2014)

The emission spectra were obtained in the range of (350 to 750) nm the excitation wavelength at 360nm and the emission one was obtained at wavelength of 439 nm, and appropriate blank corresponding to buffer were subtracted to correct background fluorescence.(Yang et al., 2013)

Quenching is the decrease of intensity of fluorescence it's classified into static and dynamic**.** Dynamic leads to no change in absorption spectra but in our work as shown in figure (4.5) and (4.6) as increasing the concentration of drugs the absorption intensity of the protein is decrease so that quenching is concern as static one.(Maltas et al., 2014)

Decreasing protein intensity with increasing of concentration indicates that the two drugs bind to protein, and that the microenvironment around the tyrosine residue was disturbed and the hydrophobicity of the residue decreased in the presence of procaine or dopamine, yet the microenvironment around the tryptophan residues had no discernable change from the binding process.(Maltas et al., 2014).

Fluorescence emission spectra of HSA with different concentration of Procaine has been drawn to get figure (4.5).

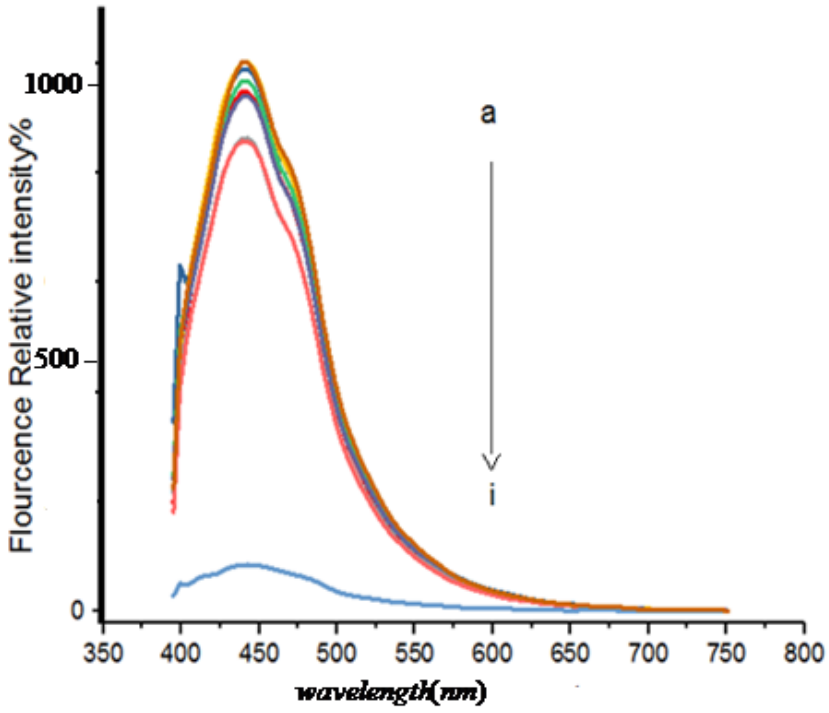

Figure4. 5: Fluorescence emission spectra of HSA in the presence of various concentration of procaine (a=Free HSA , b=0.3 mM, c= 0.4 mM, d= 0.5 mM, e=0.6mM, f= 1 mM, g= 1.2 mM, h= 2.4 mM, i=free Pro).

Fluorescence emission spectra of HSA with different concentration of Dopamine is shown in figure (4.6)

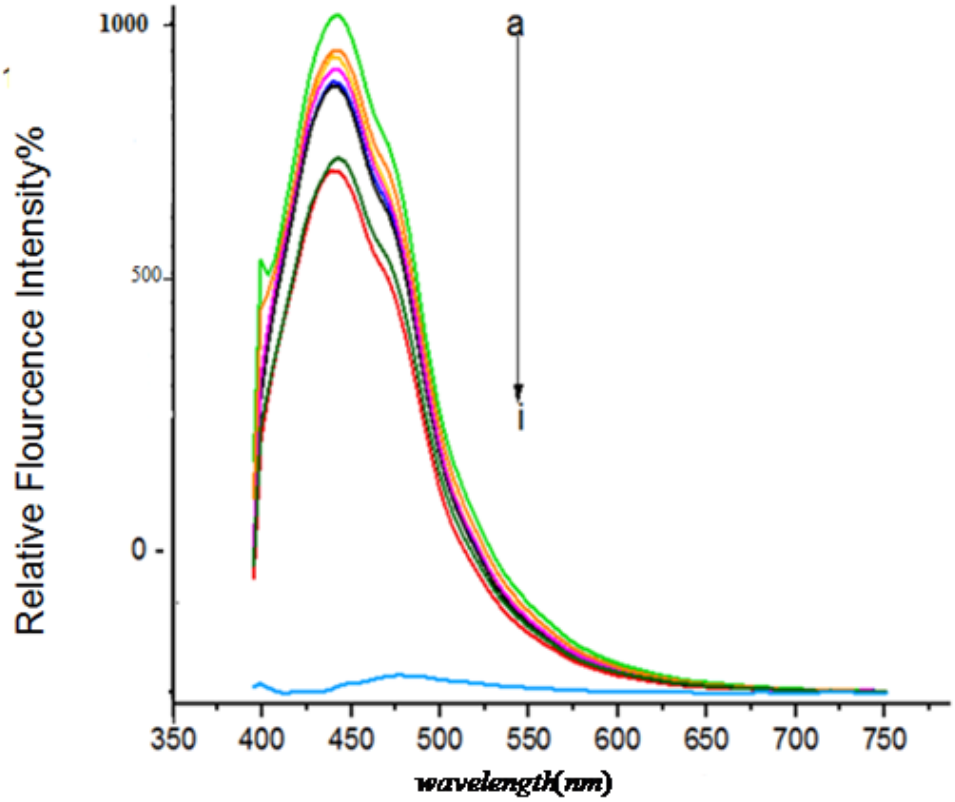

Figure4. 6: Fluorescence emission spectra of HSA in the presence of various concentration of Dopamine (a= Free HSA, b= 0.3mM, c=0.4 mM, d=0.5mM, e=0.6 mM, f=1 mM, g= 1.2mM, h= 2.4mM, i=free DA 4.8mM).

4.2.1 Stern –Volmer quenching constant (Ksv) and the quenching rate constant of the bimolecular (Kq):

Quenching is the decrease of intensity of fluorescence for given substance. Refer to any process that does that decrease. This process included excited state reactions, energy transfer, complex formation, and collisional quenching. Also, it can be produced by the binding of a molecule, known as quencher (procaine and dopamine), to the fluorescent molecule (HSA protein) from collisional encounters between the fluorophore and the quencher, this called as collisional or dynamic quenching. (Mote et al., 2010)

Stern –Volmer quenching equation is usually used to analyze the fluorescence data to get quenching parameters, this decrease of intensity of fluorescence can be described by equation (4):

$$\frac{F_0}{F} = 1 + K_q \tau_0 (\ell) = 1 + K_{sv} (\ell) \ldots\ldots\ldots (4)$$

In the above expression F_0 and F are the relative fluorescence intensities in the absence and presence of quencher, [L] is the concentration of quencher , K_{SV} is the Stern-Volmer dynamic quenching constant , k_q is the bimolecular quenching rate constant, and τ_0 is the average bimolecular lifetime in the absence of quencher . Stern –Volmer quenching constant Ksv indicates the sensitivity of the fluorophore to quencher.

4.2.1.1 Procaine's Calculations for binding quenching rate constant:

Using Stern–Volmer quenching equation calculations for determining binding quenching rate constant were determined.

Using linear regression program process linear curve has been plotted as shown in figure (4.7).

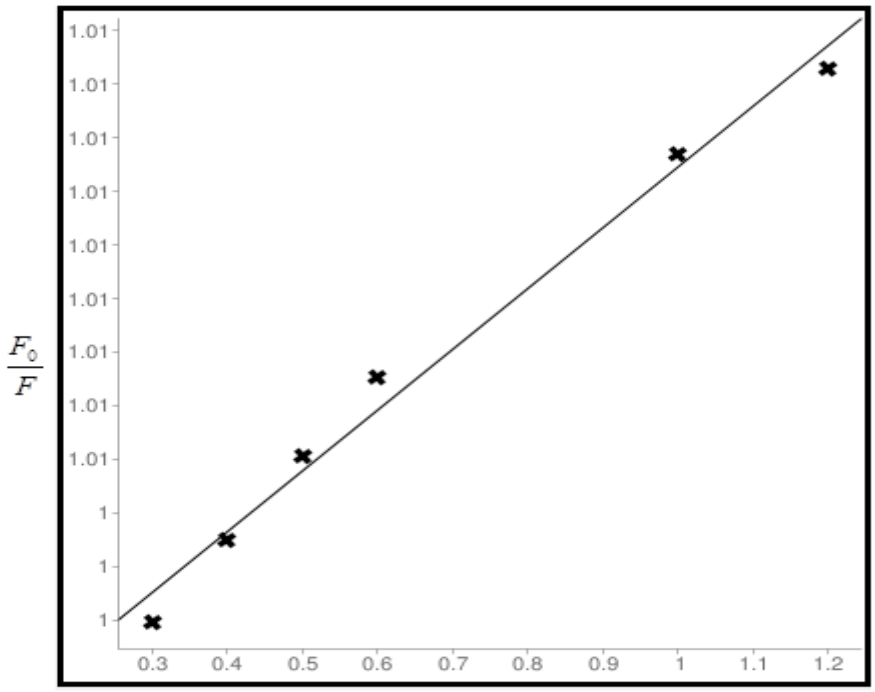

Figure4. 7: The Stern-Volmer plot for procaine –HSA complexes

Using equation (4) Stern-Volmer quenching constant Ksv assumed to be the slope of (4.7) linear figure as described in below equation.

$$Y=1.0025596+0.0056648x$$

$$\text{Slope} = 0.00566\times 10^{+3} = K_{SV} = k_q \tau_0$$

Using above relation, we can calculate the value of k_q using the fluorescence life time of 10^{-8} for HAS. (Han, 2016 , Li, 2014)

$$K_q = \frac{K_{SV}}{\tau_0} = \frac{0.00566 \times 10^3}{10^{-8}} = 0.566 \times 10^9$$

Which is smaller than the maximum dynamic quenching constant for various quenchers with biopolymer ($2 \times 10^{10}\ \ell mo\ell^{-1}s^{-1}$), (Tan, 2012).Which implies that (Wang et al.,2007)

4.2.1.2 Dopamine Calculations for binding quenching rate constant:

Using Stern–Volmer quenching equation calculations for determining binding quenching rate constant were determined.Using linear regression program process the linear curve has been plotted as shown in figure (4.8).

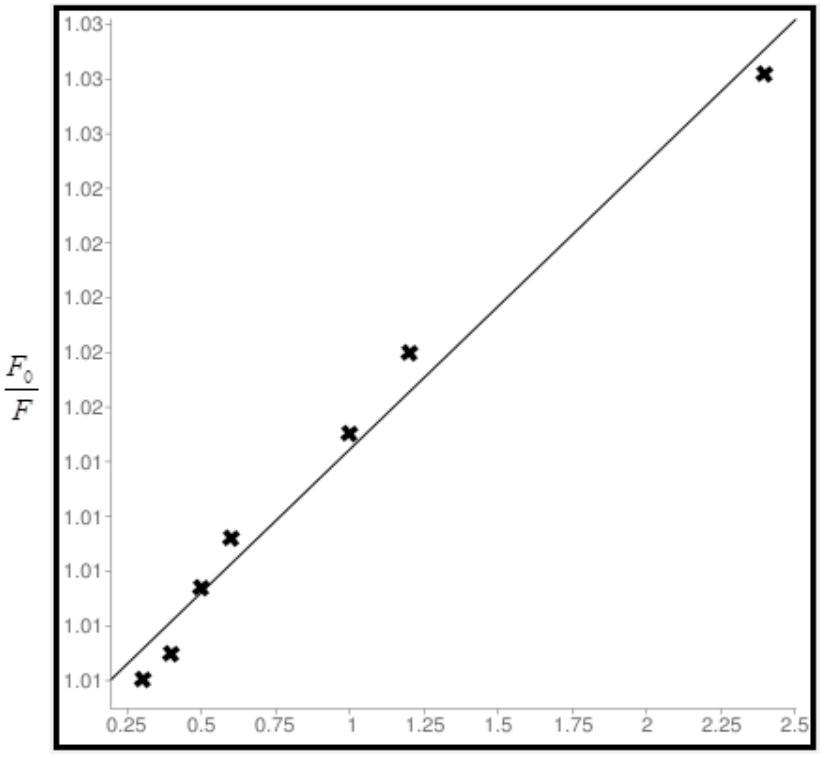

Figure4. 8: The Stern-Volmer plot for Dopamine –HSA complexes.

Stern-Volmer quenching constant Ksv was obtained by the slope of the curve obtained from figure (4.8) as described in below equation:

$$Y=1.0039834+0.0104665x$$

$$\text{Slope}= 0.0104665\times10^{3} \;=\; K_{SV} = k_q\tau_0 \; K_q = 0\cdot0104665\times10^{3}/\tau_0$$

$$K_q = \frac{0\cdot0104665\times10^{3}}{10^{-8}} = 1\cdot04665\times10^{9}$$

Previous value is smaller than the maximum dynamic quenching constant for various quenchers with biopolymer ($2\times10^{10}\,\ell mo\ell^{-1}s^{-1}$).(Wang, 2007).The value of quenching constant implies that quenching is not initiated by dynamic collision but its form contribution of static and dynamic.(Wang et al., 2007)

4.2.2 Determination of the binding constant using fluorescence spectrophotometer:

When static quenching is dominated as quenching type of fluorescence for HSA protein with two drugs the Weave -Burker can be used as equation (5). (Azimi et al., 2011)

$$\frac{1}{F_0 - F} = \frac{1}{F_0 K\ell} + \frac{1}{F_0} \quad \ldots\ldots\ldots (5)$$

Where K is the binding constant of procaine or dopamine with HSA, and can be calculated by plotting 1/ (F0-F) vs. 1/L, see figure (4.9) and figure (4.10).The value of K equals the ratio of the intercept to the slope**.**

Van der Waals interaction and hydrogen bond is the main reason for binding between the protein and two drugs. (Azimi et al., 2011).

4.2.2.1 Procaine binding constant calculations:

Calculation for binding constant of HSA-Procaine complex for different concentration of procaine have been done using equation (5) .

The binding constant K of procaine with HSA can be calculated by plotting 1/ (F0-F) vs. 1/L. Using linear regression program best linear curve was plotted as shown in figure (4.9).

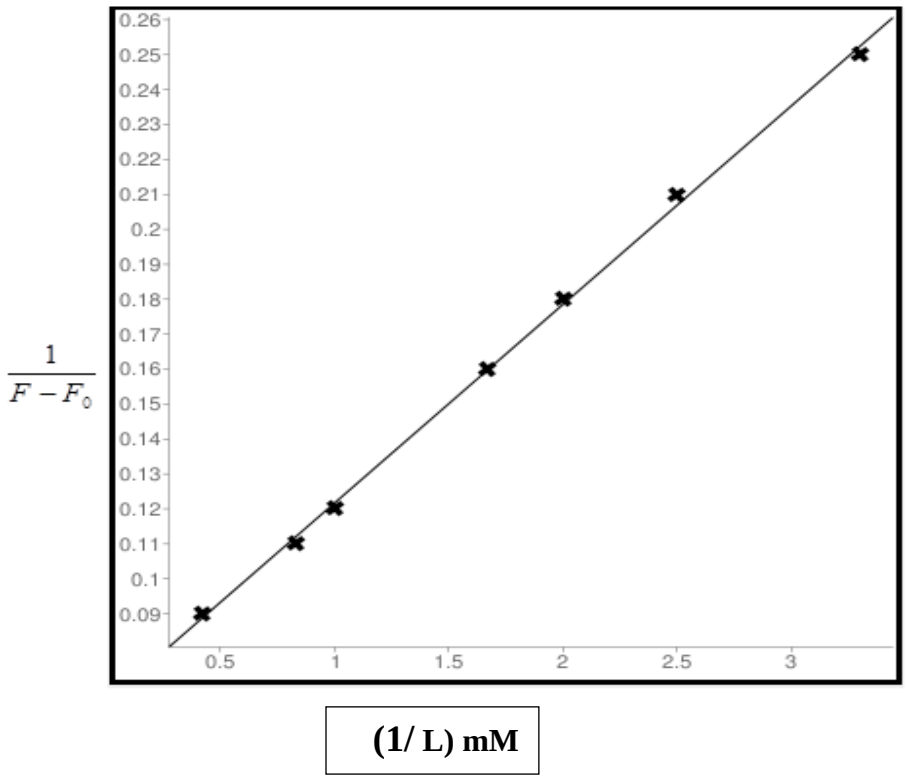

Figure4. 9: plot for 1/ (F_0-F) vs. L^{-1}

The value of K equals the ratio of the intercept to the slope.

$$y=0.06475007522974+0.056889886808176x$$

Slope= 0.056889886×10^{-3} intercept= 0. 0647500

$$K=\text{Intercept/Slope} = 1.13818\times10^{3}$$

Which nearly agree with the values obtained earlier by UV technique.

4.2.2.2 Dopamine binding constant calculations:

Calculations for determining binding constant of DA with HSA Protein has been determined using equation (5)

The binding constant K of Dopamine HSA can be calculated by plotting 1/ (F0-F) vs. 1/L. Using linear regression program linear curve has been obtained as shown in figure (4.10)

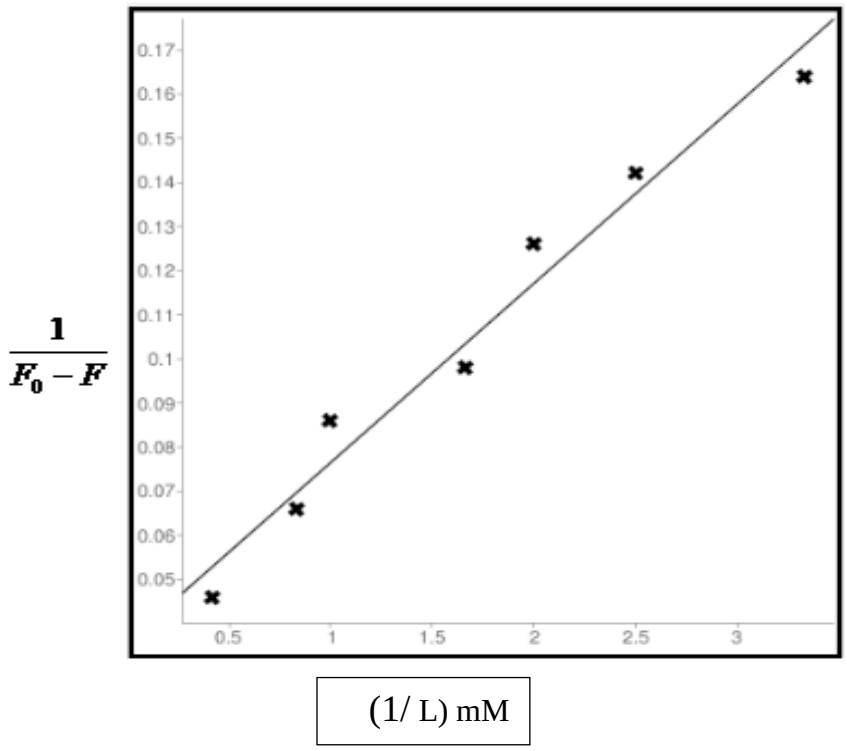

Figure4. 10: plot for 1/ (F_0-F) vs. L^{-1}

The equation of above linear curve was determined to be as described below:

$$y=0.035826+0.040655x$$

Intercept= 0.035826 Slope=0.040655×10^{-3}

$$K=\text{Intercept/Slope} = 0.88122\times10^{3}$$

Which nearly agree with the value obtained earlier by UV technique.

4.3 FT-IR Spectroscopy

FT-IR spectroscopy is a powerful technique for the study of hydrogen bonding; it has a wide spread application of qualitative and quantitative analyses in Chemistry, Biochemistry, Biology, Medicinal Chemistry and Environmental Science, it's singlemostimportantusefortheidentificationoforganiccompounds,drugsandpollutants.Now,FTIRspectroscopyisanestablishedmethodforthestructuralcharacterizationofproteins,DNAandRNA.FTIRspectroscopywithitssecondaryderivativeswasused to determine protein conformation. (Zhou et al., 2009 , MM et al., 2014)

IR spectral data including secondary structure of proteins are usually interpreted in terms of the vibrations of a structural repeat unit. These repeat units give rise to nine characteristic IR absorption bands, namely, amide A, B, and I−VII. which is a result of vibration of the groups around the peptide bond of proteins.(Kong et al., 2007)

Amide I band ranging from 1700−1600 $cm^{-1}$is the most sensitive spectral region to the protein secondary structural components, this band is due to C=O stretch vibrations of the peptide linkages (approximately 80%) , Amide II band which is much less protein conformational sensitivity than its amide I , derives mainly from in-plane NH bending (40−60% of the potential energy) and from the C-N stretching vibration (18−40%) and it's in the range of (1600-1480)cm^{-1} , while amide III band ranging from(1330 to 1220cm^{-1})is due to the C-N stretching mode coupled to the in-plane N - H bending mode .(Jackson et al., 1991)

The second derivative of the absorption spectruem of free HSA is shown in figure (4.11B) and figure (4.12B) ,where the spectra is dominated by absorbance bands of amide I and amide II at peak positions 1657 cm^{-1} and 1549 cm^{-1} for procaine's sample run ,and 1655 cm^{-1} 1540 cm^{-1} for dopamine's sample run .

Figure (4.11A), shows the spectrum of procaine HSA complexes with different concentration of Pro, and figure (4.12 A), shows the spectrum of Dopamine-HSA complexes with different concentration of dopamine. from that figure we can't assume that the relation between the concentrations of two drugs are proportional or inversely proportional to the intensity of the protein , since in this work the thickness of the samples are not the same , we try to make it homogenous as possible as we can but the surrounding environment affect and prevent that purpose, from analysis process using Fourier self-deconvolution ,second derivative ,peak positions and others we can study the change of the secondary structure of proteins after we added the drugs and see its effect .

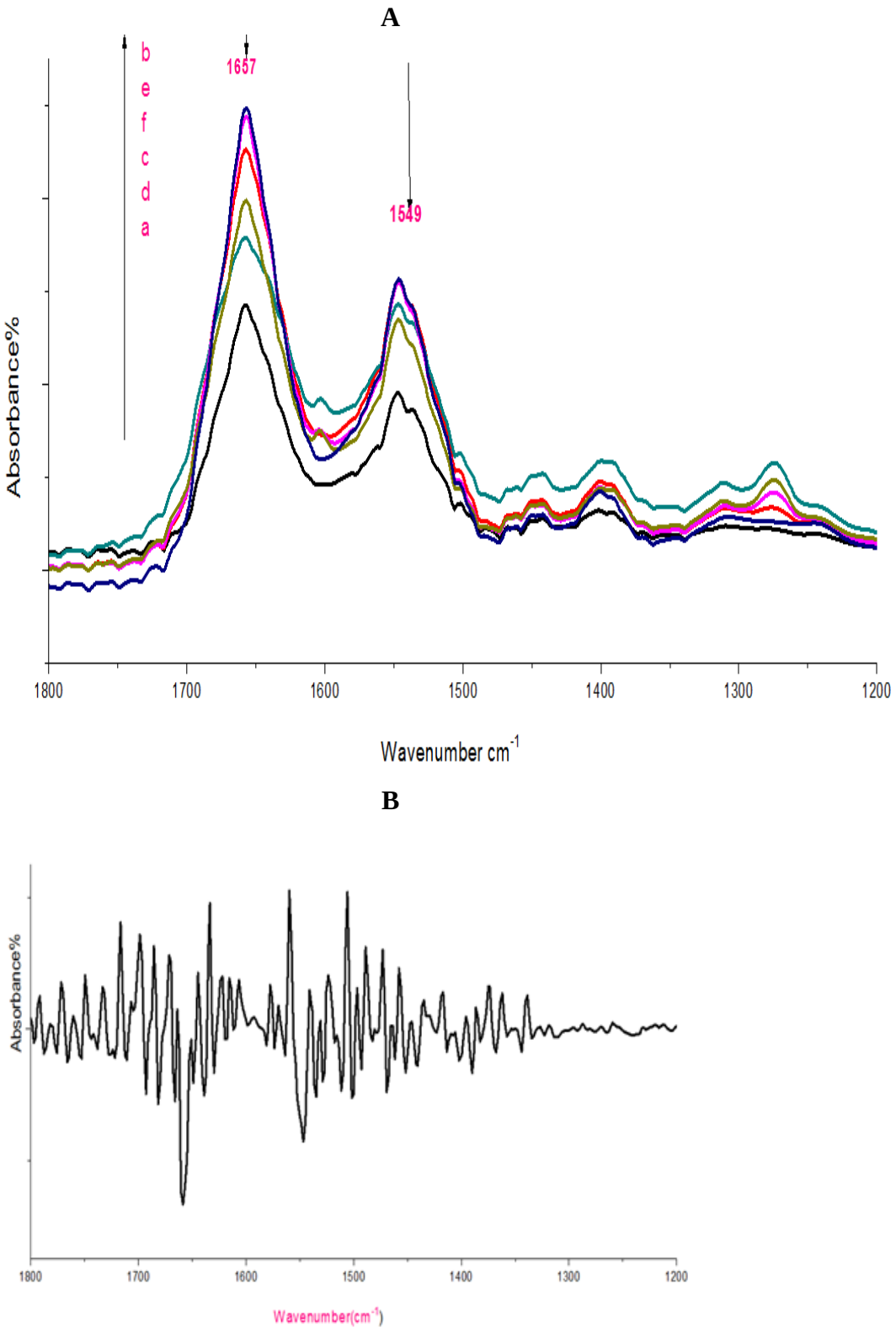

Figure4. 11:(B) The spectra of HSA free second derivative And (A) (a, b, c, d, e, f) procaine-HSA complex with concentration of (free HSA,0.15mM ,0.3mM,0.6mM,0.7 mM,0.9 mM).

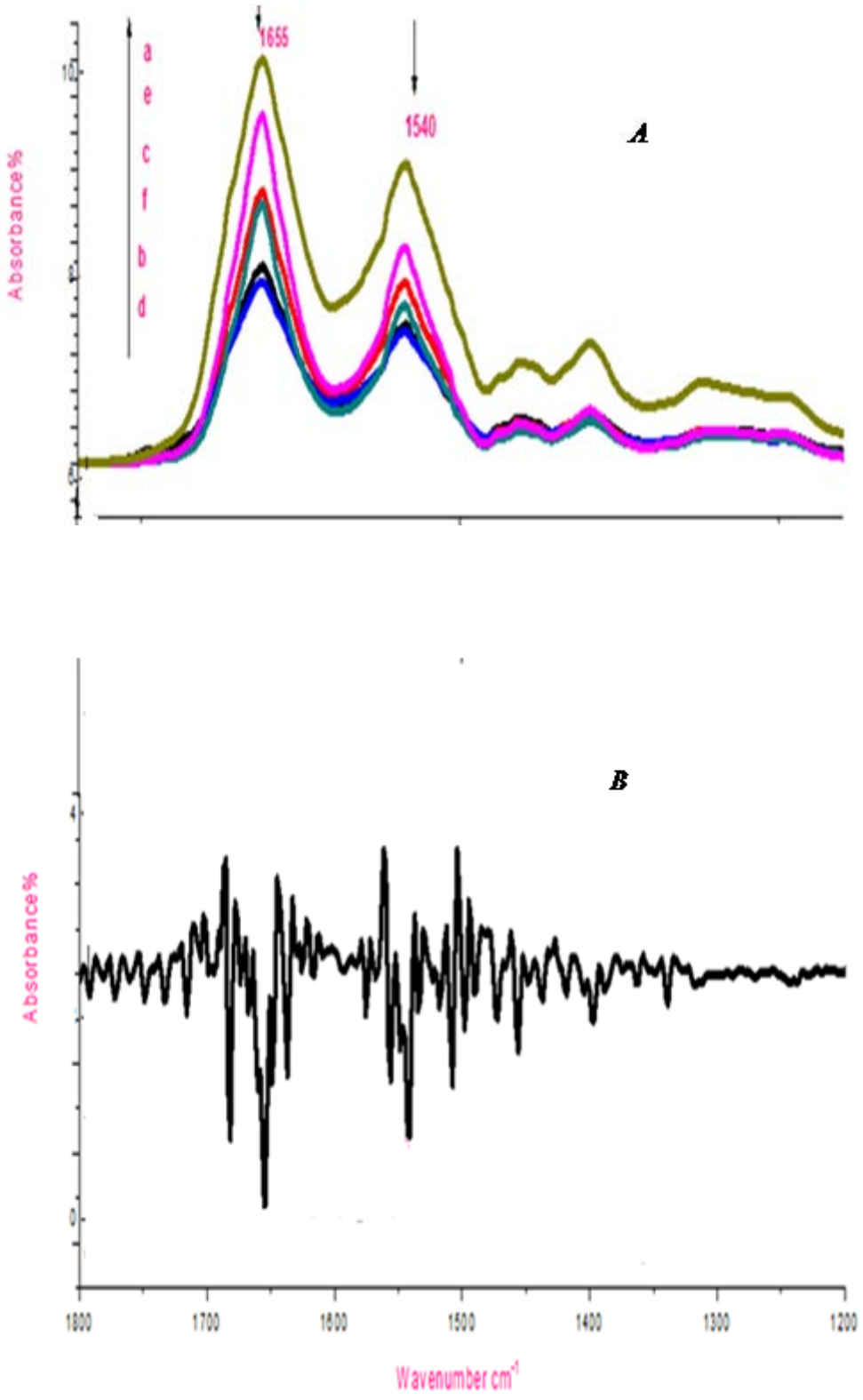

Figure4. 12:(B the lower one) The spectra of HSA free second derivative And (A the upperr one) (a, b, c, d, e, f) Dopamine-HSA complex.

Using Fourier self deconvolution and spectrum suptraction paeak postions for both HSA-Pro and HSA-DA have been displayed , the results show that there are some noticble change in the peak postions as shwon in figures (4.13 , 4.14 , 4.15 ,4.16).But in general the change are small and most of them were shift.

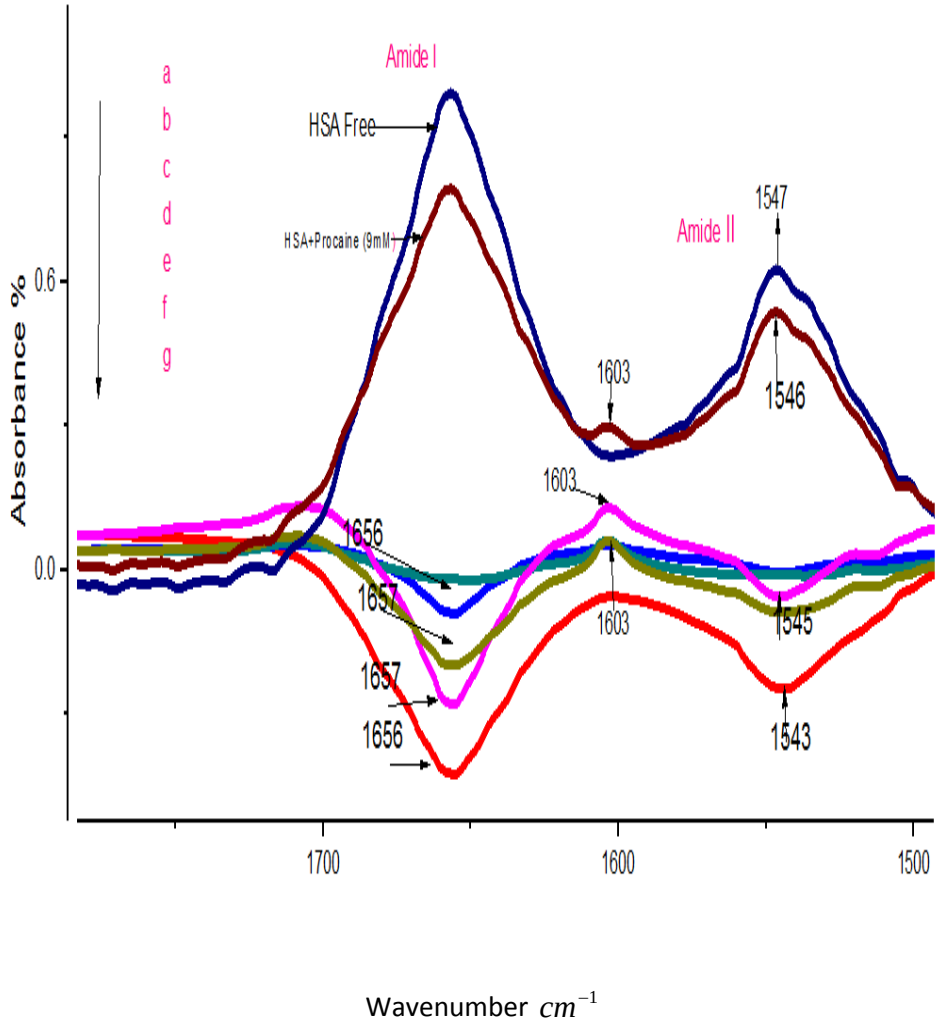

Figure4. 13: FT-IR spectra (top two curves, a and b) and differences spectra of HSA and its complexes with procaine (c, d, e, f, g) with concentration of (0.6Mm ,0.3Mm ,0.9Mm, 0.7Mm ,0.15Mm) .

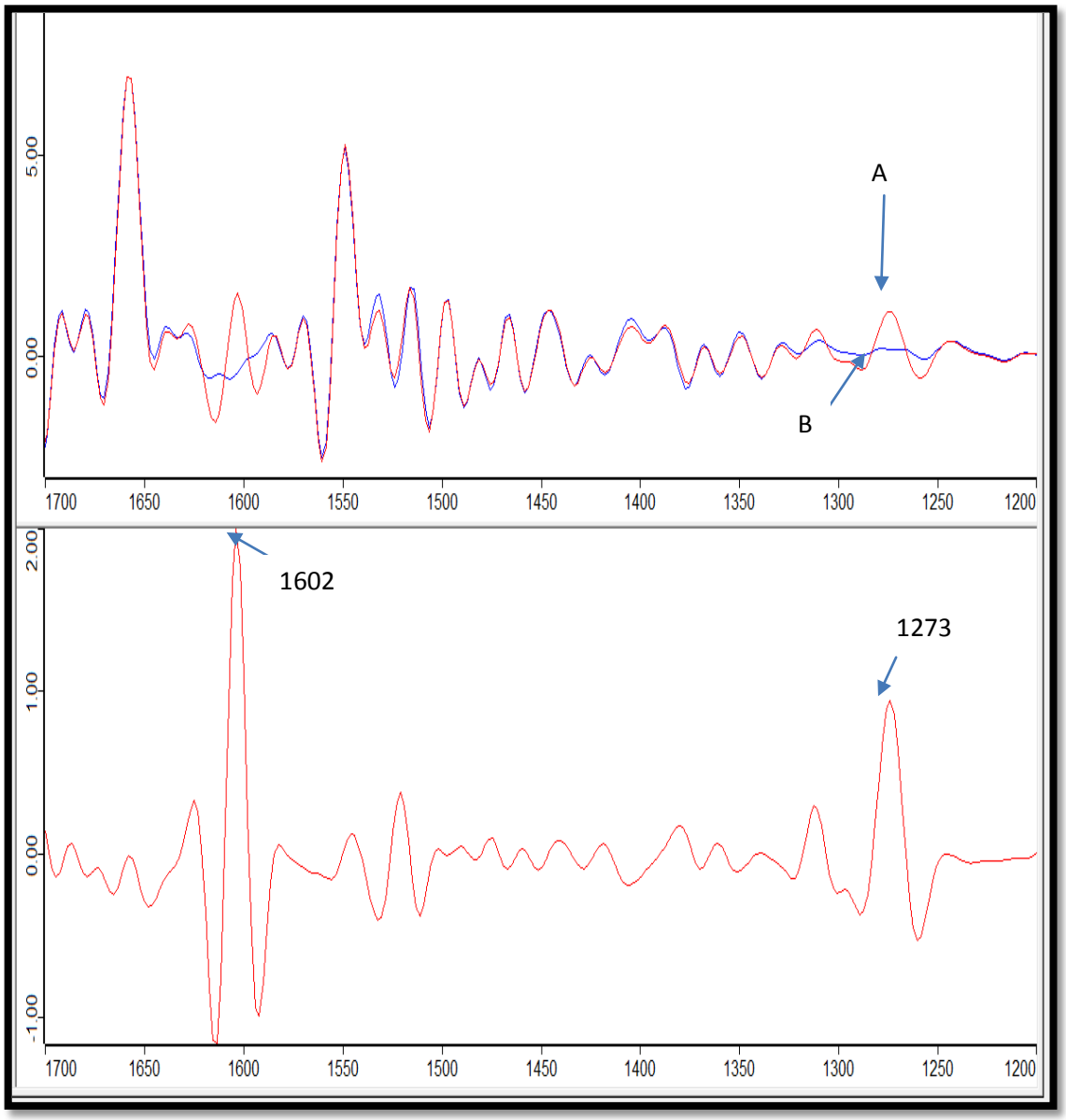

Figure4. 14: Top Part shows HSA spectra (B) and HSA-procaine 0.6mM (A)
Bottom part shows the difference Spectra between (HSA-procaine complex) – (free HSA).

For (Dopamine-HSA) interaction the results are shown in figure (4.15) and (4.16) for FT-IR spectra (top two curves) and difference spectra of HSA and its complexes with different dopamine concentrations and figure (4.16) for FSD spectra subtraction in amide I and amide II regions.

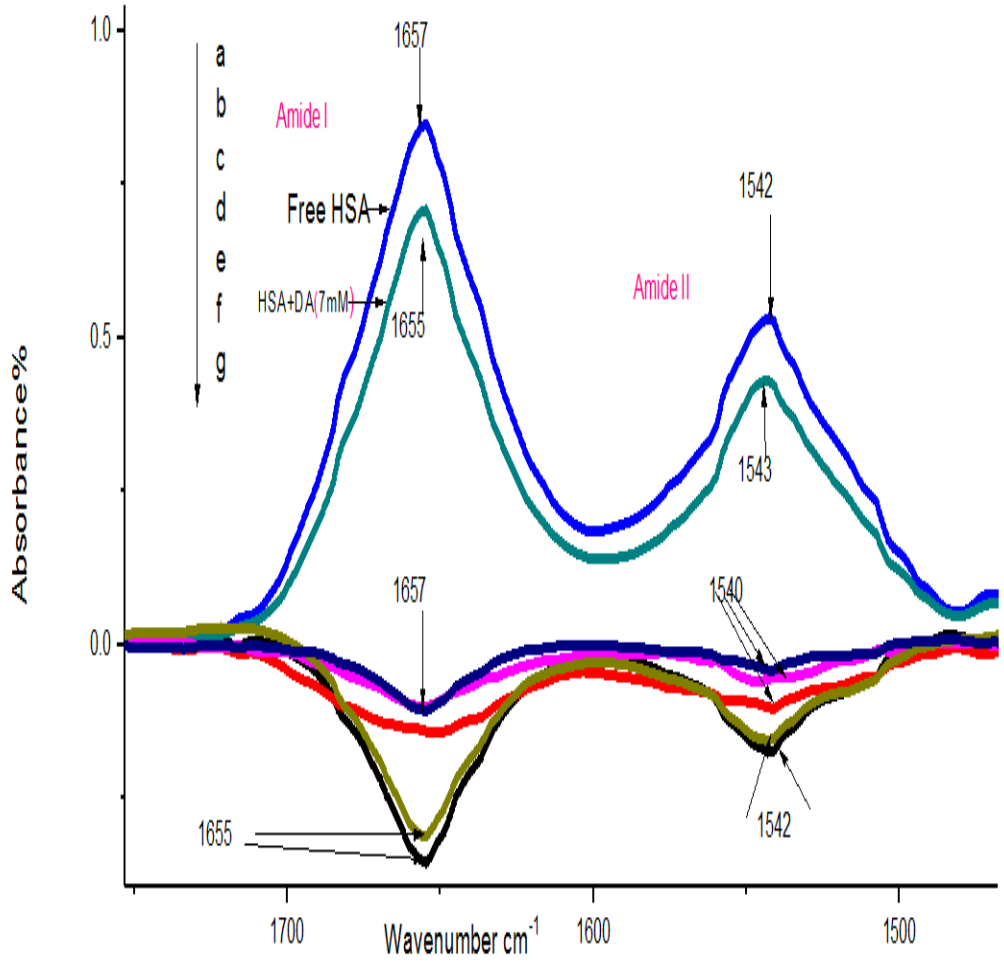

Figure4. 15: FT-IR spectra (top two curves, a and b) and differences spectra of HSA and its complexes with DA (c, d, e, f, g) with concentration of (0.4Mm ,0.3mM, 0.7Mm,0.6Mm ,0.5Mm).

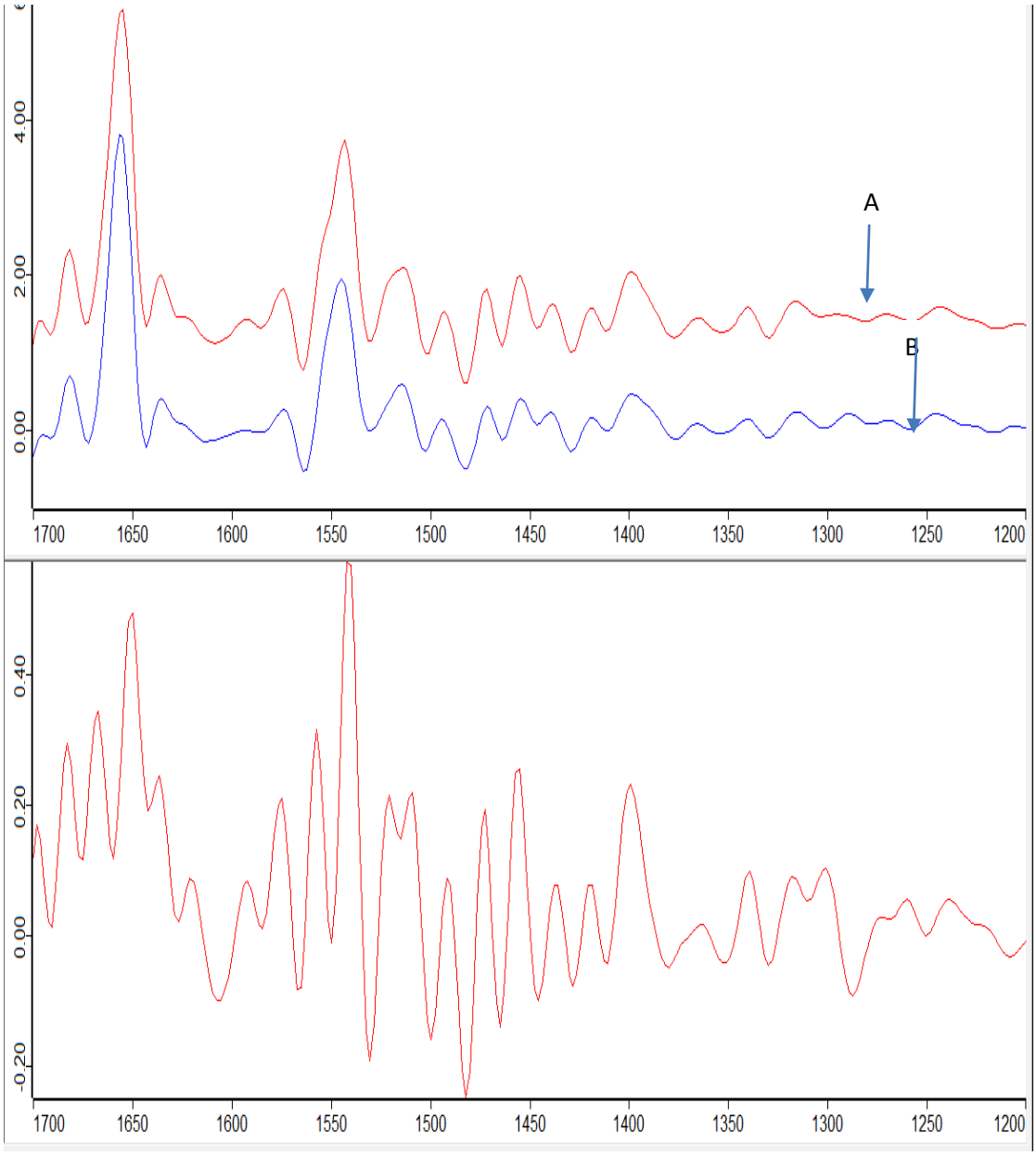

Figure4. 16: Upper Box: FSD spectra subtraction {(A) free HSA – (B) HAS- Dopamine 0.7mM), Lower Box: the result of the subtraction.

Appearance of new feature band at 1603 cm^{-1} for procaine HSA complexes, Strong negative one in amide I band, and negative feature in amide II bands for both (Pro and DA –HSA) complexes attributed that there are change in intensity of amide I and II bands which is a results of change of the secondary structure of protein after combination with drugs which due to interaction (H-Bonding) of the procaine or Dopamine with protein C=O and C-N groups. (Tajmir et al., 2007)

Using Byler and Susi procedure, determination of the secondary structure of protein and its procaine or dopamine complexes was carried out (Byler et al., 1986), in this work, quantitative analysis of the protein secondary structure in a free case and after the interaction with two drugs determined from the shape of three amides I, II, and III.

Many analysis procedures such as Fourier self-deconvolution, second derivative and integration one used to increase the spectral resolution to determine the parameters of each bands, such peak positions and area of each components of bands.

The components bands of amide I,II, and III regions were assigned to a secondary structure according to the frequency of its maximum a raised after Fourier self-deconvolution have been applied for six times .In our work for amide I band ranging from 1600 cm^{-1}- 1700 cm^{-1}assigned as follows: Both of 1606-1620 cm^{-1} and(1620 – 1633) cm^{-1}represented to β-sheets ,(1633 to 1647) cm^{-1} to random coil,1649 - 1670 cm^{-1} to α-helix,(1672-1686) cm^{-1} to turn structure , 1687-1700 cm^{-1} to β-antiparallel **.**

For amide II region ranging from 1487-1600 cm^{-1}, the absorption band assigned in the following order: Both of (1487-1506) $cm^{-1}$and (1506-1523) cm^{-1} to β-sheet ,(1523-1539) to random coil ,(1541-1558) cm^{-1} to α-helix , (1560-1577) $cm^{-1}$to turn structure ,and (1577-1594) cm^{-1} to β-antiparallel **.**

For amide III ranging from 1220-1330 cm^{-1}have been assigned as follows: 1220-1256 $cm^{-1}$to β-sheet, 1259-1287 cm^{-1} to random coil, 1288-1302 $cm^{-1}$to turn structure, and 1302-1331 $cm^{-1}$to α-helix.

Most investigations have concentrated on amid I band since it's the most sensitive one for the secondary structure change, also many studies have been reported that amide II and III one has high information contents and can be used to study the secondary structure of protein. (Tajmir-Riahi et al., 2009)

In our work the percentage of each secondary structure of HSA were calculated by normalization idea, which is integrated areas of the components bands in amide I, II, and III. Then assumed and divide by total area to get the portion of each components as described in table (4.9) and (4.10) for both HSA-Pro interaction and HSA-DA one respectively**.**

For Procaine:

Amide I:

The area for each component of amide I was determined using OPUS software program after 6 deconvolution as described in table (4.9) and figure (4.17) then we ssumed and divided by total area to get the portion of each component in that amide as shown in table (4.9).

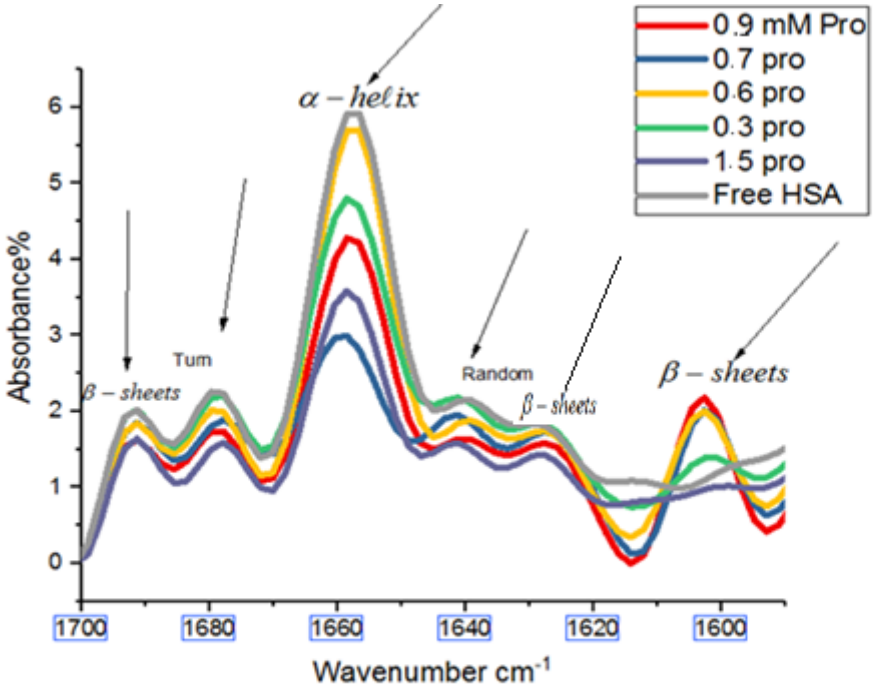

Figure4. 17: Deconvolution curve for determining bands and secondary structure for amide I

Table4. 3: Area for absorption bands for Procaine-HSA at different concentrations for amide I.

Bands	Range (cm^{-1})	[Area]	[Area]	[Area]	[Area]	[Area]	[Area]
Amide I	1700-1600	0.0	0.15mM	0.3mM	0.6mM	0.7mM	0.9mM
β-sheets	1606-1620	10.83	5.94	---	----	---	----
β-sheets	1620-1633	21.58	23.85	24.9	38.75	55.68	50.23
Random coil	1633 - 1647	34.80	26.41	29.98	37.09	34.26	28.38
α-helix	1649 - 1670	200.50	118.03	141.242	199.20	83.30	136.00
Turn Structure	1672-1686	77.45	55.25	71.99	79.46	70.29	63.55
β-sheets	1687.- 1700	85.3970	62.59	85.25	79.57	88.18	75.86

Finding total area for each concentration to get:

Total	428.55	292	353.36	435.079	331.70	354.00

Dividing each area for each concentration over the total area for that concentration the proportion of the polypeptide chain in that conformation will be described as shown in table (4.9) in amide I section and figure (4.17).

For Amide II:

We used the same procedure that has been described in amide I.

-

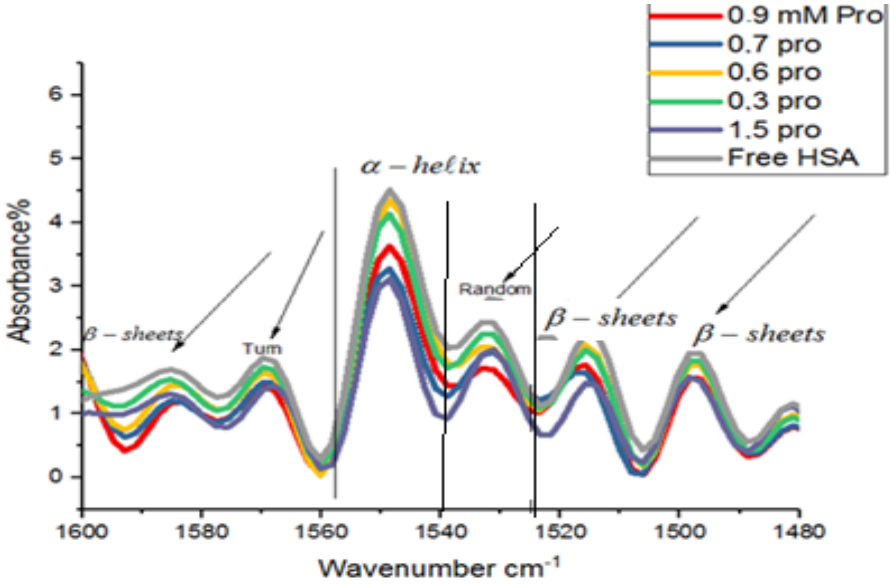

Figure4. 18: Deconvolution curve for determining bands and secondary structure for amide II.

Table4. 4: Area absorption of bands for Procaine-HSA at different concentrations for amide II

Bands	Range (cm^{-1})	[Area]	[Area]	[Area]	[Area]	[Area]	[Area]
Amide II	16001480	0.0	0.15mM	0.3mM	0.6mM	0.7mM	0.9mM
β-sheets	1487-1506	81.44	64.17	84.10	80.44	83.13	73.64
β-sheets	1506-1523	92.71	69.25	84.10	86.40	65.33	71.23
Random coil	1523 - 1539	73.47	84.00	71.00	61.80	58.74	49.36
α-helix	1541-1558	155.17	136.30	151.54	155.82	124.43	132.5
Turn Structure	1560-1577	126.00	101.91	124.49	128.91	126.21	118.49
β-sheets	1577-1594	139.57	87.18	137.00	116.26	156.79	106.85

Finding total area for each concentration to get:

Total	668.36	542.81	652.23	629.63	614.63	552.07

Dividing each area for each concentration over the total area for that concentration the proportion of the polypeptide chain in that conformationshown as described in table (4.9) in amide II section and figure (4.18).

For Amide III:

We used the same procedure to determine the portion of each component in amide III.The result is described in figure (4.19) and table (4.5).

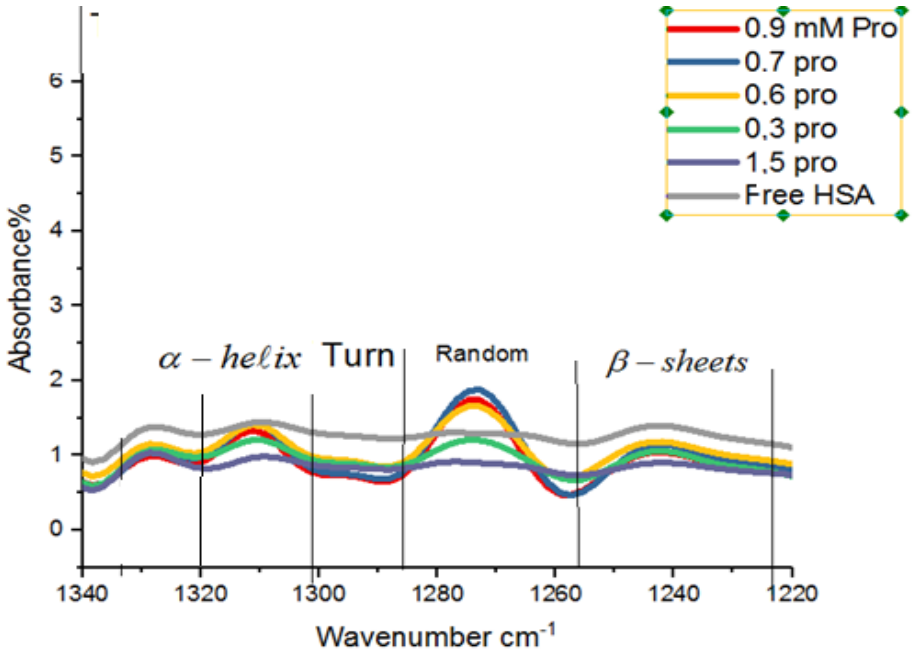

Figure4. 19: Deconvolution curve for determining range of the bands for secondary structure for amide III.

Table 4. 5: Area absorption bands for Procaine-HSA at different concentrations for amide III.

Bands	Range (cm^{-1})	[Area]	[Area]	[Area]	[Area]	[Area]	[Area]
Amide III	1320-1220	0.0	0.15mM	0.3mM	0.6mM	0.7mM	0.9Mm
β-sheets	1222-1556	13.5	7.83	14.98	16.03	19.54	16.18
Random coil	1259-1287	3.88	4.04	10.62	19.2	27.8	25.07
Turn Structure	1288 - 1302	1.41	1.04	1.57	2.33	2.84	2.82
α-helix	1302-1320	7.62	6.00	8.19	10.06	14.27	11.58

Finding total area for each concentration to get:

Total	26.41	18.91	35.36	47.62	64.45	55.65

Dividing each area for each concentration over the total area for that concentration got us the proportion of the polypeptide chain in that conformation. As described in table (4.9) in amide I section and figure (4.19).

For Dopamine:

Amide I:

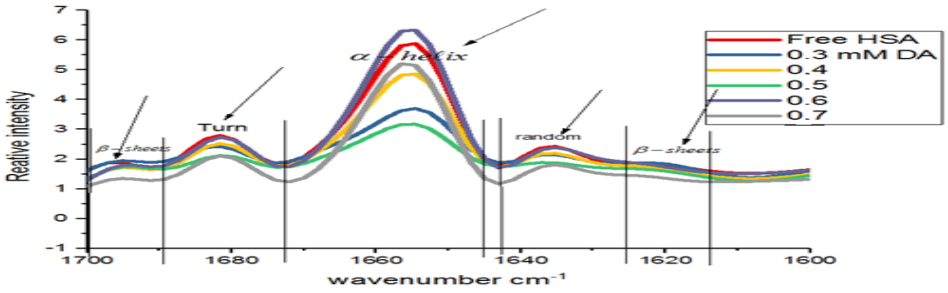

Figure4. 20: Deconvolution curve for determining range of the bands for secondary structure for amide I.

Table4. 6: Area absorption bands for DA-HSA at different concentrations for amide I.

Bands	Range (cm^{-1})	[Area]	[Area]	[Area]	[Area]	[Area]	[Area]
Amide I	1700-1600	0.0	0.3mM	0.4mM	0.5mM	0.6mM	0.7mM
β-sheets	1614-1628	3.46096	3.47132	2.66451	1.94662	1.79462	1.61238
Random coil	1628-1643	15.3878	7.62809	11.2364	4.62827	14.8481	12.4106
α-helix	1645 -1672	83.569	39.8713	64.6534	31.8005	93.1328	78.6391
Turn Structure	1674-1687	15.9181	10.6252	13.4625	9.31549	16.649	12.8315
β-sheets	1689-1700	8.4323	9.77286	8.73578	9.95985	10.7573	6.31018

Finding total area for each concentration to get:

Total	126.76	71.366	100.74	57.64	137.2	111.8

Dividing each area for each concentration over the total area for that concentration got us the proportion of the polypeptide chain in that conformation. As described in table (4.10) in amide I section and figure (4.20).

For amide II:

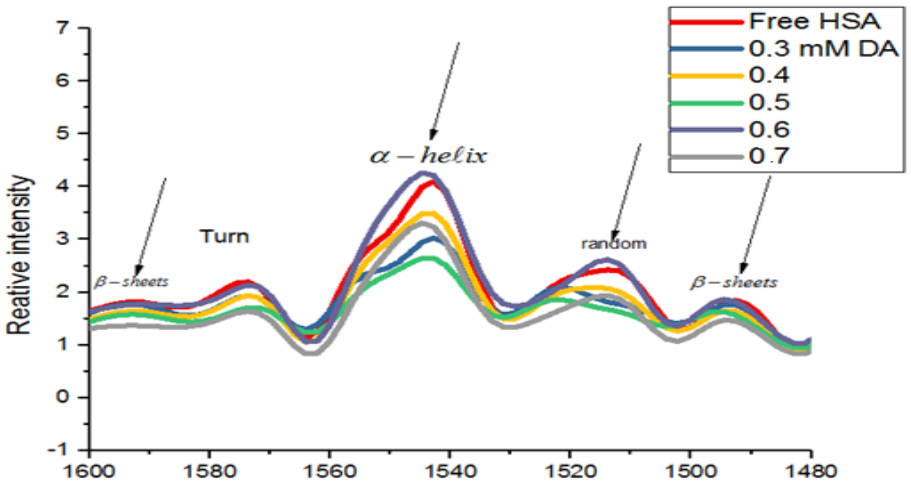

Figure4. 21: Deconvolution curve for determining range of the bands for secondary structure for amide II.

Table4. 7: Area absorption bands for DA-HSA at different concentrations for amideII.

Bands	Range (cm^{-1})	[Area]	[Area]	[Area]	[Area]	[Area]	[Area]
Amide II	1600-1480	0.0mM	0.3mM	0.4mM	0.5mM	0.6mM	0.7Mm
β-Sheet	1484-1500	25.68	15.238	18.7358	16.4326	30.27	22.4963
Random Coil	1502-1531	91.57	50.587	61.6657	32.593	69.6393	53.8371
α-helix	1533 -1564	81.75	52.730	117.869	67.1613	133.656	103.323
Turn Structure	1564 -1585	70.35	51.366	65.9504	47.1461	74.1041	53.878
β-Sheet	1585-1600	103.8	92.089	101.968	94.862	106.062	73.1984

We found total area for each concentration to get:

Total	373.18	262.008	366.189	258.19	413.7	306.73

Dividing each area for each concentration over the total area for that concentration got us the proportion of the polypeptide chain in that conformation. As described in table (4.10) in amide I section and figure (4.21).

For amide III:

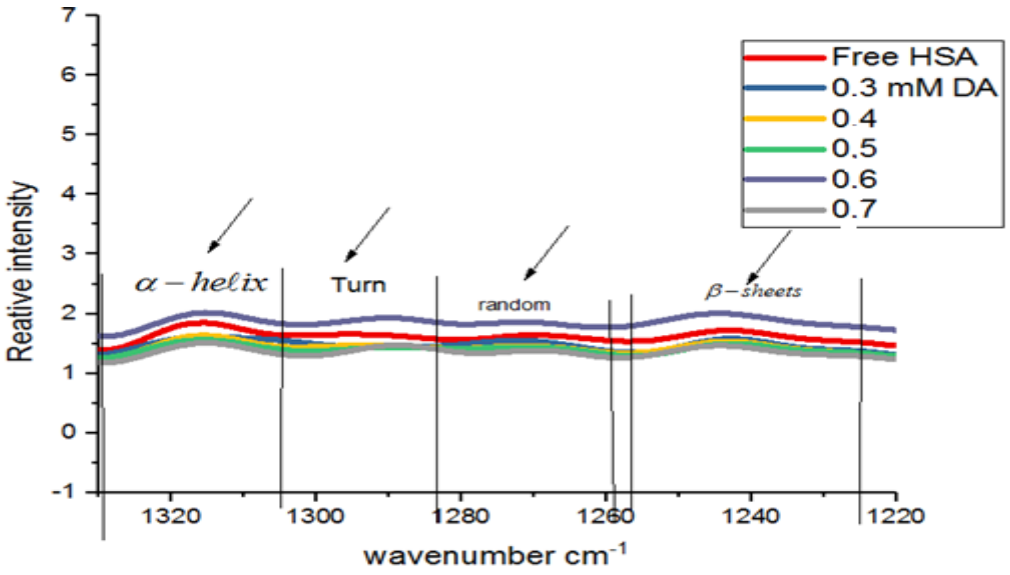

-

Figure4. 22Figure : Deconvolution curve to determining range of the bands for secondary structure of DA-HSA interaction for amide III.

Table4. 8: Area absorption bands for +DA-HSA at different concentrations for amide III

Bands	Range cm^{-1}	[Area]	[Area]	[Area]	[Area]	[Area]	[Area]
Amide III	1320-1220	0.0	0.3mM	0.4mM	0.5mM	0.6mM	0.7mM
β-sheets	1222-1255	13.49	12.298	12.95	11.32	16.00	12.83
Random coil	1257-1281	5.14	6.00	7.00	7.00	7.00	9.00
Turn Structure	1281 -1302	4.3	6.94	8.36	10.7	8.79	11.74
α-helix	1302-1317	5.99	8.76	7.8	8.69	7.67	7.77

Finding total area for each concentration:

Total	28.92	33.9	36.11	37.71	40.46	41.34

Dividing each area for each concentration over the total area for that concentration got us the proportion of the polypeptide chain in that conformation. As described in table (4.10) in amide III section and figure (4.22).

The secondary structure determination for the free HSA and its procaine or dopamine complexes, are given in (Table (4.9), and table (4.10).

Table (4.9) and table (4.10) show the content of each secondary structure of HSA before and after the interaction with procaine and dopamine at different concentration, respectively. For HSA –procaine complex it's seen that α-helix percentage decrease with the increase of procaine concentration in the calculations, and this trend is consistent in the three amide regions**.**

For procaine-HSA interaction: in amide I region HSA free consists of (20%) anti parallel β-sheet, (3%) and (5%) parallelβ-sheet, (8%) random coil, (46%) α-helical structure, and (18%) turn structure. After interaction of protein with procaine drug, α-helical structure reduces from (46%) to (39%), anti-parallel β-sheet structure increased from (20%) to (26%), while turn structure and random coil increase from (18%) to (21%) and (8%) to (10%) respectively**.**

For amide II region, HSA free consists of (12%) and (14%) parallel-β-sheet, (21%) antiparallel-β-sheet, (11%) random coil, (23%) α-helical structure, and (19%) turn structure. After interaction with procaine drug, α-helical structure increase then return back to reduce from (23%) to (20%), parallel-β-sheet increase for some concentration and return back to decrease from (14%) to (13%), turn structure increase from (19%) to (21%), and random coil decrease from (11 %) to (9%).

In amide III region HSA free consists of (51%) β-sheet structure, (15%) random coil,

(29%) α-helix and (5%) turn structure. After interaction with procaine drug, β-sheet decrease from (51%) to (29%), α-helical structure reduces from (29%) to (21%), while random coil increases from (15%) to (45%), and turn structure stay (4%) for all samples.

Table4. 9: Relative intensity of absorption bands for Procaine-HSA at different concen

Bands	Range (cm^{-1})	Intensity %	Intensity %	Intensity %	Intensity %	Intensity %	Intensity %
Amide I	**1700-1600**	**0.0**	**0.15 mM**	**0.3mM**	**0.6mM**	**0.7mM**	**0.9mM**
β-sheets	**1606-1620**	3	5	---	---	---	---
β-sheets	**1620-1633**	5	7	7	9	17	14
Random	**1633-1647**	8	8	9	9	10	8
α-helix	**1649-1670**	46	40	40	46	25	39
Turns	**1672-1686**	18	19	20	18	21	18
β-sheets	**1687-1700**	20	21	24	18	26	21
Amide II	**1600-1480**						
β-sheets	**1487 1506**	12	12	13	13	14	14
β-sheets	**1506-1523**	14	13	13	14	11	13
Random	**1523- 1539**	11	15	11	10	10	9
α-helix	**1541-1558**	23	25	23	25	20	24
Turns	**1560-1577**	19	19	19	20	21	21
β-sheets	**1577-1594**	21	16	21	18	24	19
Amide III	**1320-1220**						
β-sheets	**1222-1256**	51	41	42	34	30	29
Random	**1259-1287**	15	21	30	40	43	45
Turns	**1288--1302**	5	6	5	5	5	5
α-helix	**1302-1319**	29	32	23	21	22	21

For dopamine-HSA interaction: in amide I region HSA free consists of (3%) parallel β-sheet, (7%) antiparallel β-sheet, (12%) random, (65%) α-helical structure, (13%) turn structure. After dopamine-HSA interaction, see table (4.16), α helical structure increase from (65%) to (70%), parallel β-sheet decrease from (3%) to (1%), antiparallel β-sheet increase to (17%), both turn structure and random coil decrease from (13%) and (12%) to (11%) respectively.

For amide II region HSA free consists of (7%)parallel β-sheet ,(27%) antiparallelβ-sheet (22%) α helical structure , (25%) random coil ,and (19%) turn structure .After dopamine – HSA complexes , see table (4.16) , α helical structure increase from (22%) to (34%) ,parallel β-sheet decrease to (6%) ,antiparallel β-sheet increase from (27%) to (37%) then return to decrease to (23%) , random coil decrease from (25%) to (19%) , and turn structure reduce from (19%) to (18%).

In amide III HSA free consists of (47%) β-sheet, (20%) α-helical structure, (18%) random coil, and (15%) turn structure. After interaction with dopamine β-sheet decrease from (40%) to (30%), α helical structure increase from (20%) to (23%), random coil increases from (18%) to (20%) also turn structure increase from (15%) to (29%).

Table4. 10: Relative intensity of absorption bands for DA-HSA at different concen.

Bands	Range (cm^{-1})	Intensity %	Intensity %	Intensity %	Intensity %	Intensity %	Intensity %
Amide I	**1700-1600**	**0.0**	**0.3 mM**	**0.4mM**	**0.5mM**	**0.6mM**	**0.7mM**
β-sheets	**1614-1628**	3	5	3	3	1	1
Random	**1628-1643**	12	11	11	9	11	11
α-helix	**1645-1672**	65	56	65	55	68	70
Turns	**1674-1687**	13	14	13	16	12	11
β-sheets	**1689-1700**	7	14	8	17	8	7
Amide II	**1600-1480**						
β-sheets	**1484- 1500**	7	6	5	6	6	6
Random	**1502-1531**	25	19	17	13	18	19
α-helix	**1533- 1564**	22	20	32	26	32	34
Turns	**1564-1585**	19	20	18	18	18	18
β-sheets	**1585-1600**	27	35	28	37	26	23
Amide III	**1320-1220**						
β-sheets	**1222-1255**	47	36	36	30	39	30
Random	**1257-1281**	18	18	19	19	20	20
Turns	**1281--1302**	15	20	23	28	20	29
α-helix	**1302-1317**	20	26	22	23	21	21

The decrease of a-helix percentage with the increase of procaine and increase of it with increasing of Dopamine concentrations is evident in the calculations and this trend is nearly consistent in three Amide regions. However, β-sheet relative percentage increased with increasing procaine and decrease with increasing of dopamine concentrations.

The reduction of a-helix intensity percentage in favor of the increase of β-sheets and turn structure are believed to be due to the unfolding of the protein in the presence of procaine. Increase of a-helix intensity percentage in favor of the decrease of β-sheets are believed to be due to the folding of the protein in the presence of Dopamine as a result of the formation of H-bonding between HSA and the two drugs at C=O and C-N groups. newly H-bonding result due to a flow of electrons from the C=O to the C-N bond which decreases the intensity of the original vibrations.(Tajmair et al., 2007 , Darwish et al ., 2010)

Chapter Five: Conclusions and future work

The interaction between Procaine and Dopamine with albumin is of great interest from both the endocrinological and pharmaceutical point of view. In our work the interaction of procaine and Dopamine with HSA protein was investigated by means of UV-VIS spectrophotometer, Fluorescence spectrophotometer, andFT-IR spectroscopy.

The experimental results indicate a low binding affinity between Procaine and Dopamine with HSA protein. From analysis of the UV spectrum, the binding constants for Procaine-HAS and Dopamine-HSA are ($1.00115599\times10^{3}M^{-1}$, $0.849044\times10^{3}M^{-1}$), respectively. The analysis of the Fluorcence spectrum yield binding constants for Procaine-HAS and Dopamine-HAS interaction, that have been measured to be ($1.13818\times10^{3}M^{-1}$, $0.88122\times10^{3}M^{-1}$), respectively. The binding constant obtained by different methods has very close values. In addition, the values of Stern-Volmer quenching rate constants for both Procaine and Dopamine were measured to be (0.566×10^{9} $Lmol^{-1}s^{-1}$, 1.04665×10^{9} $Lmol^{-1}s^{-1}$), respectively. As a result, it was found that the decrease in Fluorcence intensity can be considered as the result of contribution of static and dynamic quenching, which is indicative of a complex formation between the protein with the procaine and Dopamine drugs.

Analysis of FT-IR spectrum indicated that the increasing the concentration of Procaine or Dopamine lead the unfolding of protein, change the percentage of alpha helical structure and Beta sheet .Beside that it can be inferred that the binding forces which are involved in the binding processes includes hydrophobic interactions .The newly formed H-bonding results in the C-N bond assuming partial double bond character due to a flow of electrons from the $C = O$ to C-N bond which decrease the intensity of the original vibrations.

These experimental results may be useful for drug design, and provides some important information for clinical study of drugs, since the binding between them and HAS protein is weak as described in results its suggest to carry these drugs over heterogeneous compound. And since body temperature changes during inflammatory processes ,therefore, this research need further studies such as thermodynamic (parameters (enthalpy, free energy, entropy)at different temperature to investigate the changes in the binding characteristics of procaine and Dopamine with HSA.

References:

Bäckman, L., U. Lindenberger, S.-C. Li and L. Nyberg (2010). "Linking cognitive aging to alterations in dopamine neurotransmitter functioning: recent data and future avenues." Neuroscience & Biobehavioral Reviews **34**(5): 670-677.

Bai, H. X., X. H. Liu, F. Yang and X. R. Yang (2009). "Interactions of human serum albumin with phenothiazine drugs: insights from fluorescence spectroscopic studies." Journal of the Chinese Chemical Society **56**(4): 696-702.

Bergin, R. and D. Carlström (1968). "The structure of the catecholamines. II. The crystal structure of dopamine hydrochloride." Acta Crystallographica Section B: Structural Crystallography and Crystal Chemistry **24**(11): 1506-1510.

Bhattacharya, A. A., S. Curry and N. P. Franks (2000). "Binding of the general anesthetics propofol and halothane to human serum albumin high resolution crystal structures." Journal of Biological Chemistry **275**(49): 38731-38738.

Chen, N., M. Appell, J. L. Berfield and M. E. Reith (2003). "Inhibition by arachidonic acid and other fatty acids of dopamine uptake at the human dopamine transporter." European journal of pharmacology **478**(2-3): 89-95.

Covino, B. (1986). "Pharmacology of local anaesthetic agents." British journal of anaesthesia **58**(7): 701-716.

Darwish, S. M., M. M. A. Teir, S. A. Makharza and M. M. Abu-hadid (2010). "Spectroscopic investigations of pentobarbital interaction with human serum albumin." Journal of Molecular Structure **963**(2-3): 122-129.

Hara, K. and T. Sata (2007). "The effects of the local anesthetics lidocaine and procaine on glycine and γ-aminobutyric acid receptors expressed in xenopus oocytes." Anesthesia & Analgesia **104**(6): 1434-1439.

He, W., Y. Li, C. Xue, Z. Hu, X. Chen and F. Sheng (2005). "Effect of Chinese medicine alpinetin on the structure of human serum albumin." Bioorganic & medicinal chemistry **13**(5): 1837-1845.

Kahl, S., S. Zimmermann, M. Pross, H.-U. Schulz, U. Schmidt and P. Malfertheiner (2004). "Procaine hydrochloride fails to relieve pain in patients with acute pancreatitis." Digestion **69**(1): 5-9.

Khan, S. N., B. Islam, M. Rajeswari, H. Usmani and A. U. Khan (2008). "Interaction of anesthetic supplement thiopental with human serum albumin." Acta Biochimica Polonica **55**(2): 399-409.

Kriško, A., M. Ilakovac Kveder, S. Pečar and G. Pifat (2005). "A study of caffeine binding to human serum albumin."

Li, S., D. Yao, H. Bian, Z. Chen, J. Yu, Q. Yu and H. Liang (2011). "Interaction between plumbagin and human serum albumin by fluorescence spectroscopy." Journal of solution chemistry **40**(4): 709-718.

Malamed, S. F., S. Gagnon and D. Leblanc (2001). "Articaine hydrochloride: a study of the safety of a new amide local anesthetic." The Journal of the American Dental Association **132**(2): 177-185.

Moosavi-Movahedi, Z., S. Safarian, M. Zahedi, M. Sadeghi, A. Saboury, J. Chamani, H. Bahrami, A. Ashraf-Modarres and A. A. Moosavi-Movahedi (2006). "Calorimetric and binding dissections of HSA upon interaction with bilirubin." The protein journal **25**(3): 193-201.

Racine, R., K. Livingston and A. Joaquin (1975). "Effects of procaine hydrochloride, diazepam, and diphenylhydantoin on seizure development in cortical and subcortical structures in rats." Clinical Neurophysiology **38**(4): 355-365.

Saleh, G. A., H. F. Askal, I. A. Darwish and A.-N. A. EL-SHORBAGI (2003). "Spectroscopic analytical study for the charge-transfer complexation of certain cephalosporins with chloranilic acid." Analytical Sciences **19**(2): 281-287.

Stan, D., I. Matei, C. Mihailescu, M. Savin, M. Matache, M. Hillebrand and I. Baciu (2009). "Spectroscopic investigations of the binding interaction of a new indanedione derivative with human and bovine serum albumins." Molecules **14**(4): 1614-1626.

Sugio, S., A. Kashima, S. Mochizuki, M. Noda and K. Kobayashi (1999). "Crystal structure of human serum albumin at 2.5 Å resolution." Protein engineering **12**(6): 439-446.

TAJMIR, R. H. (2007). "An overview of drug binding to human serum albumin: protein folding and unfolding."

Teir, M. A., J. Ghithan, S. Darwish and M. Abu-Hadid (2011). "Study of Progesterone interaction with Human Serum Albumin: Spectroscopic approach." Journal of Applied Biological Sciences **5**(1).

Teir, M. A., J. Ghithan, S. Darwish and M. M. Abu-Hadid (2012). "Multi-spectroscopic investigation of the interactions between cholesterol and human serum albumin." Journal of Applied Biological Sciences **6**(3): 45-55.

Ungless, M. A., E. Argilli and A. Bonci (2010). "Effects of stress and aversion on dopamine neurons: implications for addiction." Neuroscience & Biobehavioral Reviews **35**(2): 151-156.

Xie, L.-X., H.-L. Wu, C. Kang, S.-X. Xiang, X.-L. Yin, H.-W. Gu, Q. Zuo and R.-Q. Yu (2015).

"Quantitative investigation of the dynamic interaction of human serum albumin with procaine using a multi-way calibration method coupled with three-dimensional fluorescence spectroscopy." Analytical Methods **7**(16): 6552-6560.

Young, K. A., K. L. Gobrogge and Z. Wang (2011). "The role of mesocorticolimbic dopamine in regulating interactions between drugs of abuse and social behavior." Neuroscience & Biobehavioral Reviews **35**(3): 498-515.

Zhang, H., H. Bian, Q. Yu, H. Llang and Z. Chen (2008). "Interaction of sinomenine with bovine serum albumin." Int. J. Integr. Biol **4**: 21-27.

Zhang, Q., Y. Ni and S. Kokot (2012). "Binding interaction of dopamine with bovine serum albumin: A biochemical study." Spectroscopy Letters **45**(2): 85-92.

Abou-Zied, O. K. and O. I. Al-Shihi (2008). "Characterization of subdomain IIA binding site of human serum albumin in its native, unfolded, and refolded states using small molecular probes." Journal of the American Chemical Society **130**(32): 10793-10801.

Anger, P., P. Bharadwaj and L. Novotny (2006). "Enhancement and quenching of single-molecule fluorescence." Physical review letters **96**(11): 113002.

Backx, C., R. Willis, B. Feuerbacher and B. Fitton (1977). "Infrared vibration spectroscopy of molecular adsorbates on tungsten using reflection inelastic electron scattering." Surface Science **68**: 516-527.

Banwell, C. N. and E. M. McCash (1994). Fundamentals of molecular spectroscopy, McGraw-Hill New York.

Beaven, G. t. and E. Holiday (1952). Ultraviolet absorption spectra of proteins and amino acids. Advances in protein chemistry, Elsevier. **7:** 319-386.

Bhattacharya, A. A., S. Curry and N. P. Franks (2000). "Binding of the general anesthetics propofol and halothane to human serum albumin high resolution crystal structures." Journal of Biological Chemistry **275**(49): 38731-38738.

Boens, N., W. Qin, N. Basarić, J. Hofkens, M. Ameloot, J. Pouget, J.-P. Lefevre, B. Valeur, E. Gratton and M. VandeVen (2007). "Fluorescence lifetime standards for time and frequency domain fluorescence spectroscopy." Analytical chemistry **79**(5): 2137-2149.

Carter, D. C. and J. X. Ho (1994). Structure of serum albumin. Advances in protein chemistry, Elsevier. **45:** 153-203.

Černá, M., A. S. Barros, A. Nunes, S. M. Rocha, I. Delgadillo, J. Čopíková and M . A. Coimbra (2003). "Use of FT-IR spectroscopy as a tool for the analysis of polysaccharide food additives." Carbohydrate Polymers **51**(4): 383-389.

Conte, L. L., C. Chothia and J. Janin (1999). "The atomic structure of protein-protein recognition sites1." Journal of molecular biology **285**(5): 2177-2198.

Dekker, H. (1981). "Classical and quantum mechanics of the damped harmonic oscillator." Physics Reports **80**(1): 1-110.

Djukic, D., K. S. Thygesen, C. Untiedt, R. Smit, K. W. Jacobsen and J. Van Ruitenbeek (2005). "Stretching dependence of the vibration modes of a single-molecule Pt− H 2− Pt bridge." Physical Review B **71**(16): 161402.

Dulkeith, E., A. Morteani, T. Niedereichholz, T. Klar, J. Feldmann, S. Levi, F. Van Veggel, D. Reinhoudt, M. Möller and D. Gittins (2002). "Fluorescence quenching of dye molecules near gold nanoparticles: radiative and nonradiative effects." Physical review letters **89**(20): 203002.

Eftink, M. R. and C. A. Ghiron (1981). "Fluorescence quenching studies with proteins." Analytical biochemistry **114**(2): 199-227.

Ferrari, M. and V. Quaresima (2012). "A brief review on the history of human functional near-infrared spectroscopy (fNIRS) development and fields of application." Neuroimage **63**(2): 921-935.

Ferraro, J. R. and L. J. Basile (2012). Fourier transform infrared spectra: applications to chemical systems, Academic Press.

Gao, B. (1998). "Quantum-defect theory of atomic collisions and molecular vibration spectra." Physical Review A **58**(5): 4222.

Genty, B., J.-M. Briantais and N. R. Baker (1989). "The relationship between the quantum yield of photosynthetic electron transport and quenching of chlorophyll fluorescence." Biochimica et Biophysica Acta (BBA)-General Subjects **990**(1): 87-92.

Griffith, D. W. (1996). "Synthetic calibration and quantitative analysis of gas-phase FT-IR spectra." Applied spectroscopy **50**(1): 59-70.

Griffiths, P. R. and J. A. De Haseth (2007). Fourier transform infrared spectrometry, John Wiley & Sons.

Harvey, D. (2000). Modern analytical chemistry, McGraw-Hill New York.
He, X. M. and D. C. Carter (1992). "Atomic structure and chemistry of human serum albumin." Nature **358**(6383): 209.

Henderson, B. and G. F. Imbusch (2006). Optical spectroscopy of inorganic solids, Oxford University Press.

Henry, B. R. and W. Siebrand (1968). "Anharmonicity in Polyatomic Molecules. The CH-Stretching Overtone Spectrum of Benzene." The Journal of Chemical Physics **49**(12): 5369-5376.

Herzberg, G. (2013). Molecular spectra and molecular structure, Read Books Ltd.
IPNL, B. P. D., I.-L. LaMCoS and B. J. d'Alembert (2008). "Quantum and Classical Fidelity for Singular Perturbations of the Inverted and Harmonic Oscillator." arXiv preprint math-ph/0603041.

Jaggi, N. and D. Vij (2006). Fourier transform infrared spectroscopy. Handbook of Applied Solid State Spectroscopy, Springer**:** 411-450.

Janin, J. and C. Chothia (1990). "The structure of protein-protein recognition sites." J Biol Chem **265**(27).

Kačuráková, M. and R. Wilson (2001). "Developments in mid-infrared FT-IR spectroscopy of selected carbohydrates." Carbohydrate Polymers **44**(4): 291-303.

Kamentsky, L. A., M. R. Melamed and H. Derman (1965). "Spectrophotometer: new instrument for ultrarapid cell analysis." Science **150**(3696): 630-631.

Kast, S. C. T. R. E. and K. V. H. G. W. Auner (2015). "Agricultural and Environmental Management with Raman Spectroscopy."

Kerker, M. (2016). The scattering of light and other electromagnetic radiation, Elsevier.

Kos, G., H. Lohninger and R. Krska (2002). "Fourier transform mid-infrared spectroscopy with attenuated total reflection (FT-IR/ATR) as a tool for the detection of Fusarium fungi on maize." Vibrational Spectroscopy **29**(1-2): 115-119.

Kragh-Hansen, U. (1990). "Structure and ligand binding properties of human serum albumin." Danish medical bulletin **37**(1): 57-84.

Li, S., D. Yao, H. Bian, Z. Chen, J. Yu, Q. Yu and H. Liang (2011). "Interaction between plumbagin and human serum albumin by fluorescence spectroscopy." Journal of solution chemistry **40**(4): 709-718.

Magde, D., R. Wong and P. G. Seybold (2002). "Fluorescence quantum yields and their relation to lifetimes of rhodamine 6G and fluorescein in nine solvents: improved absolute standards for quantum yields." Photochemistry and photobiology **75**(4): 327-334.

Markovich, R. J. and C. Pidgeon (1991). "Introduction to Fourier transform infrared spectroscopy and applications in the pharmaceutical sciences." Pharmaceutical research **8**(6): 663-675.

Mills, I. and A. G. Robiette (1985). "On the relationship of normal modes to local modes in molecular vibrations." Molecular Physics **56**(4): 743-765.

Morris, J. V., M. A. Mahaney and J. R. Huber (1976). "Fluorescence quantum yield determinations. 9, 10-Diphenylanthracene as a reference standard in different solvents." The Journal of Physical Chemistry **80**(9): 969-974.

Najbar, J. and M. Mac (1991). "Mechanisms of fluorescence quenching of aromatic molecules by potassium iodide and potassium bromide in methanol–ethanol solutions." Journal of the Chemical Society, Faraday Transactions **87**(10): 1523-1529.

Naumann, D., D. Helm, H. Labischinski and P. Giesbrecht (1991). "The characterization of microorganisms by Fourier-transform infrared spectroscopy (FT-IR)." Modern techniques for rapid microbiological analysis: 43-96.

PALAU, J., P. ARGOS and P. PUIGDOMENECH (1982). "Protein secondary structure." Chemical Biology & Drug Design **19**(4): 394-401.

Pelton, J. T. and L. R. McLean (2000). "Spectroscopic methods for analysis of protein secondary structure." Analytical biochemistry **277**(2): 167-176.

Petitpas, I., A. A. Bhattacharya, S. Twine, M. East and S. Curry (2001). "Crystal structure analysis of warfarin binding to human serum albumin anatomy of drug site I." Journal of Biological Chemistry **276**(25): 22804-22809.

Pople, J. A. and D. L. Beveridge (1970). "Molecular orbital theory." C0., NY.

Rosén, P., H. Vogel, L. Cunningham, N. Reuss, D. J. Conley and P. Persson (2010). "Fourier transform infrared spectroscopy, a new method for rapid determination of total organic and inorganic carbon and biogenic silica concentration in lake sediments." Journal of Paleolimnology **43**(2): 247-259.

Rossel, R. V., D. Walvoort, A. McBratney, L. J. Janik and J. Skjemstad (2006). "Visible, near infrared, mid infrared or combined diffuse reflectance spectroscopy for simultaneous assessment of various soil properties." Geoderma **131**(1-2): 59-75.

Sathyanarayana, D. N. (2015). Vibrational spectroscopy: theory and applications, New Age International.

Saxena, A., R. Tripathi and R. Singh (2010). "Biological synthesis of silver nanoparticles by using onion (Allium cepa) extract and their antibacterial activity." Dig J Nanomater Bios **5**(2): 427-432.

Siesler, H. W., Y. Ozaki, S. Kawata and H. M. Heise (2008). Near-infrared spectroscopy: principles, instruments, applications, John Wiley & Sons.

Smith, B. C. (2011). Fundamentals of Fourier transform infrared spectroscopy, CRC press.

Stedwell, C. N. and N. C. Polfer (2013). Spectroscopy and the Electromagnetic Spectrum. Laser Photodissociation and Spectroscopy of Mass-separated Biomolecular Ions, Springer**:** 1-20.

Strickler, S. and R. A. Berg (1962). "Relationship between absorption intensity and fluorescence lifetime of molecules." The Journal of chemical physics **37**(4): 814-822.

Stuart, B. (2005). Infrared spectroscopy, Wiley Online Library.

Stuart, B. H. (2004). "Organic molecules." Infrared spectroscopy: Fundamentals and applications: 71-93.

Stuart, B. H. (2004). "Spectral analysis." Infrared spectroscopy: fundamentals and applications: 45-70.

Sudlow, G., D. Birkett and D. Wade (1976). "Further characterization of specific drug binding sites on human serum albumin." Molecular pharmacology **12**(6): 1052-1061.

Sudlow, G., D. J. Birkett and D. N. Wade (1975). "Spectroscopic techniques in the study of protein binding. A fluorescence technique for the evaluation of the albumin binding and displacement of warfarin and warfarin-alcohol." Clinical and Experimental Pharmacology and Physiology **2**(2): 129-140.

Sugio, S., A. Kashima, S. Mochizuki, M. Noda and K. Kobayashi (1999). "Crystal structure of human serum albumin at 2.5 Å resolution." Protein engineering **12**(6): 439-446.

Surewicz, W. K. and H. H. Mantsch (1988). "New insight into protein secondary structure from resolution-enhanced infrared spectra." Biochimica et Biophysica Acta (BBA)-Protein Structure and Molecular Enzymology **952**: 115-130.

Townes, C. H. and A. L. Schawlow (2013). Microwave spectroscopy, Courier Corporation.

Villringer, A., J. Planck, C. Hock, L. Schleinkofer and U. Dirnagl (1993). "Near infrared spectroscopy (NIRS): a new tool to study hemodynamic changes during activation of brain function in human adults." Neuroscience letters **154**(1-2): 101-104.

Wilson, K. and J. Walker (2010). Principles and techniques of biochemistry and molecular biology, Cambridge university press.

Yamasaki, K., T. Maruyama, U. Kragh-Hansen and M. Otagiri (1996).

"Characterization of site I on human serum albumin: concept about the structure of a drug binding site." Biochimica et Biophysica Acta (BBA)-Protein Structure and Molecular Enzymology **1295**(2): 147-157.

Zhu, G.-f., Y. Wang, J. Liu, H. Wang, L. Xi and L.-f. Du (2014). "Interaction between ginkgolic acid and human serum albumin by spectroscopy and molecular modeling methods." Journal of Solution Chemistry **43**(7): 1232-1249.

Zsila, F., Z. Bikádi and M. Simonyi (2003). "Probing the binding of the flavonoid, quercetin to human serum albumin by circular dichroism, electronic absorption spectroscopy and molecular modelling methods." Biochemical pharmacology **65**(3): 447-456.

Abdul-Fattah, A. M., V. Truong-Le, L. Yee, L. Nguyen, D. S. Kalonia, M. T. Cicerone and M. J. Pikal (2007). "Drying-induced variations in physico-chemical properties of amorphous pharmaceuticals and their impact on stability (I): Stability of a monoclonal antibody." Journal of pharmaceutical sciences **96**(8): 1983-2008.

Balestrieri, C., G. Colonna, A. GIOVANE, G. Irace and L. Servillo (1978). "Second-Derivative Spectroscopy of Proteins." The FEBS Journal 90(3): 433-440.

Kauppinen, J. K., D. J. Moffatt, H. H. Mantsch and D. G. Cameron (1981). "Fourier self-deconvolution: a method for resolving intrinsically overlapped bands." Applied Spectroscopy **35**(3): 271-276.

Lei, P. and J. Bauhus (2010). "Use of near-infrared reflectance spectroscopy to predict species composition in tree fine-root mixtures." Plant and soil **333**(1-2): 93-103.

Martin, R. (1994). "Spectral subtraction based on minimum statistics." power **6**: 8.
Scientific, T. (2009). NanoDrop 1000 Spectrophotometer V3. 7 User's Manual. Stand: Juli 2008.

Scientific, T. (2009). NanoDrop 3300 Fluorospectrophotometer V2. 7 User's Manual. Stand: Juli 2008

Byler, D. M., & Susi, H. (1986). Examination of the secondary structure of proteins by deconvolved FTIR spectra. *Biopolymers*, *25*(3), 469-487.

Cheng, L.-Y., Xia, W., Zhang, X., Bai, A.-M., Ouyang, Y., & Hu, Y.-J. (2017). In vitro binding comparison of cephalosporins to human serum albumin by spectroscopy and molecular docking approaches: A novel structural pursuing. *Journal of Molecular Liquids, 248*, 168-176.

(Jackson & Mantsch, 1991)Jackson, M., & Mantsch, H. H. (1991). Protein secondary structure from FT-IR spectroscopy: correlation with dihedral angles from three-dimensional Ramachandran plots. *Canadian journal of chemistry, 69*(11), 1639-1642.

Kong, J., & Yu, S. (2007). Fourier transform infrared spectroscopic analysis of protein secondary structures. *Acta biochimica et biophysica Sinica, 39*(8), 549-559

Maltas, E. (2014). Binding interactions of niclosamide with serum proteins. *journal of food and drug analysis, 22*(4), 549-555

Marty, R., N'soukpoe-Kossi, C. N., Charbonneau, D. M., Kreplak, L., & Tajmir-Riahi, H.-A. (2009). Structural characterization of cationic lipid–tRNA complexes. *Nucleic acids research, 37*(15), 5197-5207 .

Mote, U., Bhattar, S., Patil, S., & Kolekar, G. (2010). Interaction between felodipine and bovine serum albumin: fluorescence quenching study. *Luminescence, 25*(1), 1-8

Rasoulzadeh, F., Asgari, D., Naseri, A., & Rashidi, M. R. (2010). Spectroscopic studies on the interaction between erlotinib hydrochloride and bovine serum albumin. *DARU Journal of Pharmaceutical Sciences, 18*(3), 179

Stephanos, J. J. (1996). Drug-protein interactions: two-site binding of heterocyclic ligands to a monomeric hemoglobin. *Journal of inorganic biochemistry, 62*(3), 155-169

Sułkowska, A. (2002). Interaction of drugs with bovine and human serum albumin. *Journal of Molecular Structure, 614*(1-3), 227-232.

Suryawanshi, V. D., Walekar, L. S., Gore, A. H., Anbhule, P. V., & Kolekar, G. B. (2016). Spectroscopic analysis on the binding interaction of biologically active pyrimidine derivative with bovine serum albumin. *Journal of Pharmaceutical Analysis, 6*(1), 5.63-6

Tajmir-Riahi, H., N'Soukpoe-Kossi, C., & Joly, D. (2009). Structural analysis of protein–DNA and protein–RNA interactions by FTIR, UV-visible and CD spectroscopic methods. *Journal of Spectroscopy, 23*(2), 81-101 .

Tan, M., Liang, W., Luo, X., & Gu, Y. (2012). Fluorescence spectroscopy study on the interaction between evodiamine and bovine serum albumin. *Journal of Chemistry, 2013* .

Wang, Y.-Q., Zhang, H.-M., Zhang, G.-C., Tao, W.-H., & Tang, S.-H. (2007). Interaction of the flavonoid hesperidin with bovine serum albumin: A fluorescence quenching study. *Journal of luminescence, 126*(1), 211-218 .

Yang, G.-D., Li, C., Zeng, A.-G., Zhao, Y., Yang, R., & Bian, X.-L. (2013). Fluorescence spectroscopy of osthole binding to human serum albumin. *Journal of Pharmaceutical Analysis, 3*(3), 200-204 .

Zhong, W., Wang, Y., Yu, J.-S., Liang, Y., Ni, K., & Tu, S. (2004). The interaction of human serum albumin with a novel antidiabetic agent—SU-118. *Journal of pharmaceutical sciences, 93*(4), 1039-1046

Zhou, B., Zhang, Z., Zhang, Y., Li, R., Xiao, Q., Liu, Y., & Li, Z. (2009). Binding of cationic porphyrin to human serum albumin studied using comprehensive spectroscopic methods. *Journal of pharmaceutical sciences, 98*(1), 105-113

Azimi, O., Emami, Z., Salari, H., & Chamani, J. (2011). Probing the interaction of human serum albumin with norfloxacin in the presence of high-frequency electromagnetic fields: Fluorescence spectroscopy and circular dichroism investigations. *Molecules,*

تأثيرات تفاعل المخدر الموضعي (بروكايين) والناقل العصبي (دوبامين) مع بروتين الدم البشري من خلال التحليل الطيفي

إعداد: رانية عبد الجليل سليمان فقيات

إشراف: د. موسى ابو طير

الملخص:

إن التوزيع وعمليات الأيض لكثير من العناصر البيولوجية في الجسم سواء كانت أمصال أو منتجات طبيعية،مرتبطة بقدرة هذه العناصر على الإرتباط مع بروتين الدم البشري(HSA) ،اذ أن دراسة ارتباط مثل هذه الجزيئات مع بروتين الدم البشري حتمي وله أهم يةأساسية .دراسات واسعة النطاق على جوانب مختلفة لتفاعل بروتين الدم البشري مع الأمصال لا تزال في التقدم لأهمية هذه الدراسات في العمليات العلاجية.

في هذه الدراسة تم دراسة تأثير المخدر الموضوعي الذي يستخدم بالعمليات الجراحية (Pro) والناقل العصبي في الجهاز العصبي المركزي للثديات (DA)مع بروتين الدم البشري (Human Serum (Albumin عند درجة الحموضة الفسيولوجية ،باستخدام جهاز مطياف الأشعة فوق البنفسجية (UV-VIS (spectrophotometer وجهاز الإشعاع(Fluorcence Spectrophotometer) وجهاز مطياف تحويل فوريير للأشعة تحت الحمراء (FT-IR).

أظهرت النتائج أن شدة إمتصاص الأشعة الفوق بنفسجية لبروتين الدم تزداد بزيادة نسب البروكين وكذلك الدوبامين مع ثبات تركيز البروتين . ومن طيف الأشعة الفوق بنفسجية تم حساب ثابت الترابط والقيم هي (1.0085×10^3)للبروكين و (0.849044×10^3) للدوبامين.

ومن خلال تحليل الإشعاع المنبعث،أستنتج أن البروكيين والدوبامين لهما القدرة على خفض شدة الإشعاع المنبعث ذاتيا من بروتين الدم البشري من خلال تداخل ما بين الية (Static and Dynamic quenching).

ايضا من خلال طيف الغشعاع المنبعث تم إيجاد ثابت الترابط وهو (1.1188×10^3) للبروكين و(0.88122×10^3) للدوبامين مع بروتين الدم البشري،من الواضح أن هذه القيم تتناسب مع القيم التي تم الحصول عليها لثابت الترابط من جهاز مطياف الأشعة فوق البنفسجية.

باستخدام جهاز مطياف تحويل فوريير للأشعة تحت الحمراء مع تطبيق تقنية (Fourier Self-deconvolution) و (Second Derivative) بالإضافة الى تقنية (Peak picking) تم تحليل مناطق اميد واحد وأميد اثنان وأميد ثلاثة في بروتين الدم البشري لتحديد بنية البروتين الثانوية (Secondary Structure) والية ارتباط البروكين والدوبامين مع بروتين الدم،لقد لوحظ أنه مع زيادة تراكيز البروكيين أو الدوبامين إلى بروتين الدم فإن شدة حزم الإمتصاص تقل وهذا يدل على حدوث التفاعل .ايضا جميع القمم تم تحديدها عند عدة نسب من البروكيين أو الدوبامين بالمقارنة مع بروتين الدم البشري .

إضافة إلى ذلك أظهر الطيف المقاس بواسطة جهاز مطياف تحويل فوريير للاشعة تحت الحمراء أن البنية الثانوية لبروتين الدم البشري،تغيرت نتيجة إضافة نسب من البروكيين والدوبامين ، الذي أظهر تغيير واضح على نسب شدة الإمتصاص الممثلة ل (α-helix)بالمقارنة مع مع حزم الإمتصاص الممثلة ل (β-sheets) , هذا التباين والإختلاف في الشدة يرجع الى تكوين الروابط الهيدروجينية (H-Bonding) في الجزيئات المعقدة ، وهو ما يفسر الميول الذاتي لكل من (α-helix) و (β-Sheets)لتكوين هذه الروابط .